


Genetic analysis argues for a coactivator function for the *Saccharomyces cerevisiae* Tup1 corepressor

Emily J. Parnell,¹ Timothy J. Parnell,² and David J. Stillman ^{1,*}

¹Department of Pathology, University of Utah Health Sciences Center, Salt Lake City, UT 84112, USA

²Bioinformatics Shared Resource, Huntsman Cancer Institute, University of Utah, Salt Lake City, UT 84112, USA

*Corresponding author: Email: david.stillman@path.utah.edu

Abstract

The Tup1-Cyc8 corepressor complex of *Saccharomyces cerevisiae* is recruited to promoters by DNA-binding proteins to repress transcription of genes, including the a-specific mating-type genes. We report here a *tup1(S649F)* mutant that displays mating irregularities and an α -predominant growth defect. RNA-Seq and ChIP-Seq were used to analyze gene expression and Tup1 occupancy changes in mutant vs wild type in both a and α cells. Increased Tup1(S649F) occupancy tended to occur upstream of upregulated genes, whereas locations with decreased occupancy usually did not show changes in gene expression, suggesting this mutant not only loses corepressor function but also behaves as a coactivator. Based upon studies demonstrating a dual role of Tup1 in both repression and activation, we postulate that the coactivator function of Tup1(S649F) results from diminished interaction with repressor proteins, including $\alpha 2$. We also found that large changes in mating-type-specific gene expression between a and α or between mutant and wild type were not easily explained by the range of Tup1 occupancy levels within their promoters, as predicted by the classic model of a-specific gene repression by Tup1. Most surprisingly, we observed Tup1 occupancy upstream of the a-specific gene *MFA2* and the α -specific gene *MF(ALPHA)1* in cells in which each gene was expressed rather than repressed. These results, combined with the identification of additional mating-related genes upregulated in the *tup1(S649F)* α strain, illustrate that the role of Tup1 in distinguishing mating types in yeast appears to be both more comprehensive and more nuanced than previously appreciated.

Keywords: gene regulation; chromatin; coactivator; corepressor

Introduction

Regulation of gene expression at complex promoters is facilitated by a host of factors, including sequence-specific DNA-binding factors and proteins that are recruited as coactivators or corepressors. Some of these complexes, including SAGA and Sin3/Rpd3, modify the amino-terminal tails of histones to promote either activation or repression (Wolffe 1996; Ng and Bird 2000; Verdone *et al.* 2005; Shahbazian and Grunstein 2007; Soffers and Workman 2020). Others are nucleosome remodelers that move or evict nucleosomes, such as SWI/SNF and Isw2 (Lin *et al.* 2020; Markert and Luger 2021; Reyes *et al.* 2021). A balance of activating and repressing functions is required to maintain appropriate gene expression levels, and increasing evidence points to an integration of these two processes. Some multiprotein complexes can affect transcription either positively or negatively, suggesting their roles may be context-dependent rather than fitting within strict categories (Kliewe *et al.* 2017; Adams *et al.* 2018).

The Tup1-Cyc8 complex of *Saccharomyces cerevisiae* was one of the first to be identified as a transcriptional corepressor (Keleher *et al.* 1992; Tzamarias and Struhl 1994). This 1.2 megadalton complex consists of a 4:1 ratio of Tup1 to Cyc8 (Williams *et al.* 1991; Varanasi *et al.* 1996). Neither protein binds DNA directly, but when tethered upstream of a heterologous reporter, Tup1 and

Cyc8 can confer repression (Tzamarias and Struhl 1994). Tup1-Cyc8 is recruited to native promoters by DNA-binding proteins, thereby repressing diverse groups of genes including cell-type-specific genes (a haploid vs α haploid vs diploid), glucose- and hypoxia-regulated genes, as well as genes that respond to osmotic stress or DNA damage and genes involved in flocculation (Lipke and Hull-Pillsbury 1984; Malave and Dent 2006). In total, Tup1-Cyc8 affects the expression of approximately 300–500 genes in budding yeast (Derisi *et al.* 1997; Green and Johnson 2004; Chen *et al.* 2013). Both Tup1 and Cyc8 have sequence homologs in *Schizosacchaomyces pombe* and *Caenorhabditis elegans* as well as evolutionary relatives in higher eukaryotes, such as Groucho in *Drosophila melanogaster* and TLE1 in humans (Chen and Courey 2000). Metazoan members of the Groucho/TLE family of corepressors have similar domain structures and corepressor functions as Tup1 and regulate genes that are essential to many developmental pathways or are implicated in various cancers (Fisher and Caudy 1998; Grbavec *et al.* 1998; Parkhurst 1998; Grbavec *et al.* 1999; Chen and Courey 2000).

The C-terminus of Tup1 folds into a WD domain with seven repeats that form the blades of a propeller-like structure (Williams and Trumbly 1990). This protein–protein interaction domain binds to the homeodomain-containing protein $\alpha 2$, the

Received: June 23, 2021. Accepted: July 20, 2021

© The Author(s) 2021. Published by Oxford University Press on behalf of Genetics Society of America. All rights reserved.

For permissions, please email: journals.permissions@oup.com

repressor of α -specific genes via $\alpha 2$ /Mcm1 and of haploid-specific genes via $\alpha 1/\alpha 2$ (Johnson and Herskowitz 1985; Keleher et al. 1989; Dranginis 1990; Komachi et al. 1994). Deletion of the WD domain is effectively a *tup1* null, and mutations within the WD domain affect target genes other than the $\alpha 2$ -regulated genes, suggesting it interacts with additional DNA-binding factors or proteins required for repression (Williams and Trumbly 1990; Carrico and Zitomer 1998). The N-terminus of Tup1 facilitates its tetramerization as well as the interaction of tetramers with Cyc8 (Jabet et al. 2000). The central portion of the protein contains two additional domains with repressive functions, with the more C-terminal domain playing a more substantial role (Tzamaris and Struhl 1994; Zhang et al. 2002). Cyc8 has 10 tandem repeats of a tetratricopeptide repeat sequence motif, capable of interacting with diverse proteins, including Tup1 (Smith et al. 1995; Tzamaris and Struhl 1995; Gounalaki et al. 2000). The combination of Tup1 and Cyc8 thus provides ample diverse surfaces for interaction with proteins, allowing them to be recruited in a range of different contexts to affect the expression of a large number of genes.

A number of mechanisms for Tup1-Cyc8 repression have been proposed, including recruitment of histone deacetylases, formation of compact nucleosomal arrays, as well as interference with the Mediator complex and/or RNA Polymerase II itself (Smith and Johnson 2000; Malave and Dent 2006). These possibilities are not mutually exclusive, and it seems likely that distinct, possibly redundant mechanisms operate at different promoters (Zhang and Reese 2004). A potential unifying model for Tup1-Cyc8 repression suggests that it masks the activation domains of its many DNA-binding recruiter proteins, thereby preventing the association of many recruiters with coactivator proteins (Wong and Struhl 2011). In this model, the DNA-binding proteins that associate with Tup1-Cyc8 would be capable of recruiting both coactivators and the Tup1-Cyc8 corepressor. Environmental conditions could prompt release from the repressed, masked state, possibly by a post-translational modification or a conformational change of either the DNA-binding protein or Tup1-Cyc8.

Several studies support the conclusion that Tup1-Cyc8 can function as more than a simple corepressor. Tup1 associates with some of its target promoters during gene activation as well as during repression, in some cases even facilitating recruitment of coactivators such as SAGA and SWI/SNF (Papamichos-Chronakis et al. 2002; Proft and Struhl 2002; Mennella et al. 2003; Desimone and Laney 2010). Tup1's continued presence throughout induction may be important for priming these promoters for subsequent reactivation following repression. At some glucose-repressed genes, Tup1 is responsible for Htz1 deposition at the promoter-proximal nucleosome, a mark that is needed for rapid recruitment of Mediator and activation following Tup1-Cyc8-mediated repression (Gligoris et al. 2007). Similarly, at the repressed promoters of mating-type-specific genes, Gcn5 acetylation of histone H3 amino-terminal tails requires Tup1-Cyc8 (Desimone and Laney 2010). In these cases, Tup1 appears to repress transcription while also providing a chromatin state that allows for a rapid switch back to activation. A coactivator function of Tup1 has been observed at additional genes, including those encoding tryptophan and other amino acid transporters, the BAP2 amino acid permease gene, the CIT2 citrate synthase gene, the FRE2 plasma membrane ferric reductase gene, and the FLO11 flocculation gene (Conlan et al. 1999; Nielsen et al. 2001; Fragiadakis et al. 2004; Tanaka and Mukai 2015; Nguyen et al. 2018).

The picture emerging from studies of Tup1-Cyc8 is that the complex would be most aptly termed a transcriptional "coregulator." The persistence of Tup1-Cyc8 association as promoters is activated following repression suggests there is a functional switch that converts the complex from a corepressor to a coactivator. Understanding these two functions of Tup1-Cyc8 is complicated by the fact that the complex appears to play different roles at subsets of promoters. It has also become increasingly clear that Tup1-Cyc8 target promoters have multiple, redundant mechanisms of recruitment, with binding sites for distinct DNA-binding proteins that are each capable of recruiting Tup1 and/or Cyc8. Using different combinations of these binding sites, promoters are able to repress transcription in response to different environmental conditions (Hanlon et al. 2011; Tam and van Werven 2020). Some Tup1-Cyc8 association sites cannot be explained by the current list of recruiter proteins, suggesting that additional DNA-binding proteins that recruit Tup1-Cyc8 have yet to be identified.

We recently identified the Ash1 DNA-binding repressor protein as an additional Tup1 recruiter (Parnell et al. 2020). Ash1 is necessary for daughter cell-specific repression of the *HO* gene, which encodes the endonuclease that cleaves the *MAT* locus to allow haploid yeast cells to switch mating type (Strathern et al. 1982; Bobola et al. 1996; Sil and Herskowitz 1996). The *HO* promoter is highly regulated, utilizing multiple coactivators and corepressors. Recruitment of Tup1 to *HO* by Ash1 occurs in an activator-dependent manner and may be important for resetting the promoter for repression following a brief burst of gene activation at the end of the G1 phase of the cell cycle (Parnell et al. 2020). Ash1 colocalizes with Tup1 at a number of other genomic sites, suggesting it recruits Tup1 to additional promoters.

Our discovery of Tup1 repression of the *HO* promoter in haploid cells resulted from a genetic screen for negative regulators of the *HO* promoter (Parnell and Stillman 2019). In this screen, we identified a *tup1* hypomorph, *tup1*(H575Y), which allowed some expression of *HO* in the absence of its pioneer transcription factor, Swi5. Here we report new, targeted screens to identify additional *tup1* alleles, with the goal of better understanding the role of Tup1, both at the *HO* promoter and genome-wide. RNA-Seq and chromatin immunoprecipitation (ChIP)-Seq experiments with the *tup1*(S649F) mutant identified in this new screen provide evidence suggesting that Tup1 has a coactivator as well as a corepressor function and that this dichotomy of function is not restricted to a small number of genes but is a general feature of Tup1 regulation. Our study also provides new insight into the role of Tup1 at the mating-type-specific genes, some of the prototypical genes that first suggested the corepressor function of the Tup1-Cyc8 complex.

Methods

Strain and plasmid construction

Yeast strains are listed in Supplementary Table S1 and are isogenic in the W303 background (*leu2-3,112 trp1-1 can1-100 ura3-1 ade2-1 his3-11,15*; Thomas and Rothstein 1989). Standard strain construction methods were used (Rothstein 1991; Sherman 1991; Knop et al. 1999; Storici et al. 2001). Further details concerning plasmid and strain construction are available upon request.

For the genetic screens, *tup1* null strains were constructed by PCR amplification of either *HIS3MX* from pFA6:*HIS3MX6* (Longtine et al. 1998) or *URA3:KanMX* from pCORE with *Kluyveromyces lactis* *URA3* and *KanMX4* (Storici et al. 2001), followed

by integration at the *TUP1* locus to replace the open reading frame (ORF) [*tup1*($\Delta+1$ to +2142)].

A *TUP1* YCp TRP1 plasmid (M5765) was constructed by inserting a 3.5-kb PstI-HindIII fragment from plasmid pFW45 (Williams and Trumbly 1990) containing the *TUP1* ORF as well as 237 bp upstream and 1074 bp downstream endogenous sequence into YCplac22 TRP1 (Gietz and Sugino 1988). To facilitate the construction of *tup1* mutant alleles on plasmids, a pUC57 plasmid containing wild-type *TUP1* with three translationally silent restriction sites (SmaI, XmaI at amino acids 585–587, NruI at amino acids 636–637, and EcoRI at amino acids 675–677) was synthesized by Genewiz. PCR amplified fragments containing the relevant portions of mutant *tup1* plasmids isolated from genetic screens were cloned into the *TUP1* pUC57 vector and then used to replace wild-type *TUP1* in the *TUP1* YCp plasmid.

Endogenous *tup1* alleles were constructed by replacement of the *URA3(K.L)::KanMX* cassette in DY18163 [*MATa tup1*($\Delta+1$ to +2142)::*URA3(K.L)::KanMX*] with a PstI-HindIII fragment containing *TUP1* and flanking sequences from plasmids containing the relevant alleles. The mutant alleles inserted at the native *TUP1* locus were verified by PCR analysis and by sequencing. These *tup1* endogenous alleles were unmarked and were subsequently followed in crosses by qPCR, detecting the *Tm* difference between wild-type and mutant products from primers spanning the introduced silent EcoRV restriction site in mutant alleles (Wittwer et al. 2003).

The *TUP1*-V5 and *tup1*(S649F)-V5 alleles were constructed as described (Knop et al. 1999) by PCR amplifying and C-terminally integrating a V5 epitope tag with a *HIS3MX* marker from pZC03 (pFA6a-TEV-6xGly-V5-HIS3MX), provided by Zaily Connell and Tim Formosa (plasmid #44073; Addgene). Tagging of *TUP1* imparted a slight flocculation phenotype, and tagging of *tup1*(S649F) increased the severity of its flocculation phenotype.

Genetic screens

Genetic screens for *tup1* mutants were conducted in *swi5 ash1* and *gcn5* mutant backgrounds using strains DY18884 [*MAT α* HO-ADE2 HO-CAN1 *swi5::KanMX ash1::LEU2 ade2::HphMX tup1*($\Delta+1$ to +2142)::*HIS3MX*] and DY19135 [*MATa* HO-ADE2 HO-CAN1

gcn5::HIS3 ade2::HphMX tup1($\Delta+1$ to +2142)::*URA3(K.L)::KanMX*], in which the *TUP1* ORF was replaced with a marker cassette. Strains were cotransformed with a mutagenized *TUP1* PCR product, whose primers introduced complementarity to the cotransformed linearized YCplac22 vector, allowing the formation of complete plasmids containing *tup1* mutations via homologous recombination (Muhlrad et al. 1992), and mutants were selected on SD-Ade-Trp plates. For each screen, multiple *TUP1* PCR reactions were transformed and plated separately to allow for later determination of the independence of mutant alleles. Transformation of a wild-type *TUP1* plasmid (M5765) was always performed and plated separately for comparison purposes, as restoration of wild-type *TUP1* function from the plasmid allowed for better growth and a weak Ade⁺ phenotype relative to the starting *tup1* null strain. Seven candidate mutants were selected from each transformation, often of different sizes and ranging in color from pink to white, as ADE2 expression affects colony color. All were then retested for growth on SD-Ade-Trp in comparison with a wild-type *TUP1* plasmid.

Candidate mutants from the *swi5 ash1* screen were initially verified by isolation of the mutant *tup1* plasmid, followed by retransformation into the original *swi5 ash1 tup1 HO-ADE2* strain and retesting of the growth phenotype on SD-Ade-Trp media. For those that maintained an Ade⁺ phenotype, plasmid DNA was isolated and subjected to Sanger sequencing using a series of primers that covered the *TUP1* gene. A large proportion of mutants that were retested displayed strong growth, demonstrating that the screen was very effective, with a low false positivity rate. Therefore, when performing the screen in the *gcn5* mutant, we quickly narrowed our interest to those mutant positions that appeared in multiple *tup1* plasmids or in both screens without retesting each to confirm its phenotype. The extent to which the mutants in Table 1 were verified is indicated by their “Classification.” Many additional mutants were obtained from both screens but are not listed if they were observed in only one plasmid or were not independently retested for increased HO-ADE2 expression. These include, but are not limited to: C348R (*gcn5* screen), I676M (*swi5 ash1* screen), and Y580H (*swi5 ash1* screen); these positions are noted due to their correspondence

Table 1 *Tup1* mutants obtained from genetic screens for activation of HO expression

AA position	WT AA	Mutant AA	# Indep mutants	Classification ^a	Screen	Position within WD	Structural information
445	Y	C	2	3	<i>gcn5</i>	DA Loop 1-2	Top surface previously identified
526 ^b	E	G	2	3	<i>swi5 ash1</i>	DA Loop 3-4	Top surface
560	F	S, Y	2	3	<i>swi5 ash1</i>	CD Loop 4th	Side surface
564	R	G	2	3	<i>swi5 ash1</i>	D Sheet 4th	Side surface
* 565	L	P	2	1,2	<i>swi5 ash1</i>	D Sheet 4th	Just under side surface
566	D	G	3	1,2	<i>swi5 ash1</i>	DA Loop 4-5	Side surface
569	N	D, K	2	3	<i>swi5 ash1</i>	DA Loop 4-5	Not in structure
570	E	G, K, V	6	3	<i>swi5 ash1</i>	DA Loop 4-5	Not in structure
* 575	H	P, R, Y	7	1,2	<i>swi5 ash1, gcn5</i>	DA Loop 4-5	Just under top surface
* 597	D	G, N, Y	12	1,2	<i>swi5 ash1</i>	BC Turn 5th	Top surface
602	L	P	2	3	<i>gcn5</i>	C Sheet 5th	
629	H	R, Y	2	3	<i>swi5 ash1, gcn5</i>	DA Loop 5-6	Just under top surface
649	S	F	2	3	<i>gcn5</i>	B Sheet 6th	Just under top surface
* 673 ^b	N	D	15	3	<i>swi5 ash1</i>	DA Loop 6-7	Top surface previously identified
699	D	G	3	1,2	<i>swi5 ash1, gcn5</i>	BC Turn 7th	Top surface
* 700	C	R, Y	2	1,2	<i>swi5 ash1</i>	BC Turn 7th	Top surface

^aClassification designation is as follows:

1 = Single mutation; verified by re-transformation of mutant plasmid and confirmation of phenotype.

2 = Mutation position is identical to a single, verified mutation. However, this mutant either has additional positions that are mutated or was not verified.

3 = Mutation was identified in more than one mutant, but none are both single and verified.

^bMutation position is identical to one previously identified by Komachi and Johnson (1997).

An asterisk in the first column indicates alleles that were constructed at the endogenous locus and tested in Figure 2.

with mutations identified by [Komachi and Johnson \(1997\)](#) that affected the interaction of Tup1 with $\alpha 2$.

Growth assays

For plate spot dilution assays, liquid cultures of the indicated strains were grown to saturation, serially diluted in 10-fold increments, spotted onto YPAD media for the number of days indicated, and photographed.

Immunoblot analysis

Cells were grown at 30°C in YPA medium (1% yeast extract, 2% bactopectone, and 0.002% adenine) supplemented with 2% dextrose ([Sherman 1991](#)) to an OD₆₆₀ of 1.0–1.5. For each sample, 1.0 OD of cells was collected, and protein lysate was prepared by pulverizing cells with glass beads in sodium dodecyl sulfate buffer. Standard methods for sodium dodecyl sulfate-polyacrylamide gel electrophoresis (SDS-PAGE) were used. A nitrocellulose membrane (Bio-Rad) was used for western transfer with standard methods. Immunoblots were incubated with a 1:5000 dilution of mouse monoclonal antibody to the V5 epitope (SV5-Pk1; Abcam) or a 1:10,000 dilution of mouse monoclonal antibody to Pgk1 (Invitrogen), followed by a 1:10,000 dilution of sheep anti-mouse antibody conjugated to horseradish peroxidase (GE Biosciences). Antibody signals were detected with Super Signal West Dura Chemiluminescent Substrate (Thermo Scientific).

RNA expression and ChIP analysis

Cells for RNA isolation or ChIP were grown at 30°C in YPA medium (1% yeast extract, 2% bactopectone, and 0.002% adenine) supplemented with 2% dextrose ([Sherman 1991](#)) to an OD₆₆₀ of 0.6–to 0.8.

RNA was isolated and *HO* mRNA levels were measured by reverse transcription-quantitative PCR (RT-qPCR), as described previously ([Voth et al. 2007](#)). *HO* RNA expression was normalized to that of *RPR1*, the RNA component of RNase P, transcribed by RNA polymerase III. *RPR1* transcription is not usually affected by genetic manipulations that alter RNA Pol II transcription.

ChIPs were performed as described ([Bhoite et al. 2001](#); [Voth et al. 2007](#)), using mouse monoclonal antibody to the V5 epitope (SV5-Pk1; Abcam) and antibody-coated magnetic beads (Pan Mouse IgG beads; Life Technologies). Cells were cross-linked in 1% formaldehyde overnight at 4°C and quenched with 125-mM glycine. For ChIP qPCR experiments in [Figure 6A](#), the concentration of ChIP DNA at the relevant target gene was normalized to its corresponding Input DNA and a No Tag control.

Quantitative PCR (qPCR) experiments for RNA expression and ChIP analysis were conducted on a Roche Lightcycler 480 or a ThermoFisher QuantStudio 3. Concentrations were determined using wild-type complementary DNA or input ChIP DNA for in-run standard curves via the E-method ([Tellmann 2006](#)). The Student's t-test was used to determine significance levels, as reported in the figure legends. Primers used for RT-qPCR and ChIP qPCR are listed in [Supplementary Table S2](#).

RNA-Seq analysis

RNA was prepared as described ([Ausubel 1987](#)) and column purified using the QIAGEN RNeasy Mini Kit. Libraries were prepared for triplicate samples from each strain using the Illumina TruSeq Stranded Total RNA Ribo-zero Gold Library Prep reagent kit. Sequencing was performed on an Illumina NovaSeq 6000 as 50-bp paired-end runs (University of Utah High Throughput Genomics Facility). Fastq files were de-duplicated of optical duplicates using BBmap clumpify (version 38.34) and optical

distance of 10,000, trimmed of adapters using Cutadapt (version 2.8) with minimum overlap length (option -O) of 6 and minimum output length (option -m) of 20, and aligned to the genome (UCSC sacCer3) using the STAR aligner (version 2.7.3) with basic two-pass mode. Read counts over transcripts were collected using subRead featureCounts (version 1.6.3) using custom transcript annotation that includes untranslated regions (UTRs) and excludes dubious annotation ([Parnell 2021b](#)). Differential analysis was performed with DESeq2 with the aid of the hciR package ([Parnell 2021a](#)). Differential genes that were selected by Custom heat maps were made with pHeatmap and volcano plots with ggPlot in custom R scripts.

Only protein-coding genes were considered for quantitation of genes that demonstrated changes in gene expression ([Figure 5A](#)), and any with a base mean of less than 30 were eliminated. Genes counted in [Figure 5A](#) had a log₂ fold expression change of greater than +1.0 or less than -1.0 (twofold change). For the Tup1 occupancy ChIP-Seq vs RNA expression RNA-Seq correlations in [Figure 7, B and D](#), and [Supplementary Figures S4–S6](#), any changes greater than +0.585 or less than -0.585 (1.5-fold change) were counted.

ChIP-Seq analysis

Chromatin isolated from individual, independently collected Tup1-V5 or Tup1(S649F)-V5 cell pellets was used for multiple ChIPs, performed as described above, which were then pooled for each replicate. Libraries were prepared for triplicate ChIP samples and a single input sample for each strain using the New England Biolabs NEBNext ChIP-Seq Library Prep Reagent Set with dual index primers. Sequencing was performed with an Illumina NovaSeq 6000, 50-bp paired-end run in two lanes (University of Utah High Throughput Genomics Facility). Fastq files were aligned to the genome (UCSC sacCer3) using Novocraft Novoalign version 4.2.2, giving primer adapters for trimming, Novaseq tuned parameters, and allowing for 1 random, multihit alignment. Alignments from individual sequencing runs were merged for each sample. An average of 13 million fragments was mapped.

Samples were then processed with MultiRepMacsChIPSeq pipeline version 14.1 ([Parnell 2020](#)). Alignments over mitochondrial, 2-micron, rDNA, and telomeric regions were discarded from the analysis. Excessive duplicate alignments (range 7–16%) were randomly subsampled to a uniform 6% for each sample after removing optical duplicates (minimum pixel distance of 10,000). Replicates were depth-normalized, averaged together, and peak calls generated with a minimum length of 250 bp, gap size of 50 bp, and minimum *q*-value statistic of 3. Alignment counts from each replicate were collected for each peak and used for correlation metrics and identifying differentially occupied peaks by running DESeq2, version 1.28 ([Love et al. 2014](#)). Peaks were annotated by intersection using bedtools ([Quinlan 2020](#)) with interval files of either genes or intergenic regions. Heat maps were generated by first collecting data with BioToolBox get_relative_data from the peak midpoint 25 windows of 25 bp, and plotting the data using pHeatmap ([Kolde 2020](#)) in custom R scripts.

Peaks that were annotated as “Intergenic,” as described above, with a flanking feature of a tRNA, other Pol III gene (*SCR1*, *RPR1*) or snRNA, were individually examined in the IGV genome browser (Broad Institute) to determine whether the peak overlapped the tRNA/snRNA or whether the peak was located in the intergenic region between a tRNA/snRNA and another gene. Peaks overlapping tRNA/snRNA genes were classified as “Poll III, snRNA” and the peaks between tRNA/snRNA and/or Pol II

Table 2 Location of Tup1 peaks relative to genes that change greater than twofold in the *tup1(S649F)* mutant relative to WT

Location of Tup1 peak relative to gene ^a	No. of genes that increase expression	No. of genes that decrease expression	Total genes with expression changes
(B) Strains with mating-type α			
(A) Strains with mating-type α			
Upstream ^b	280 (78%)	6 (29%)	286 (75%)
Over the ORF	3 (1%)	4 (19%)	7 (2%)
No peak ^c	77 (21%)	11 (52%)	88 (23%)
Total	360 (100%)	21 (100%)	381 (100%)
Upstream ^b	374 (67%)	9 (56%)	383 (66%)
Over the ORF	12 (2%)	1 (6%)	13 (2%)
No peak ^c	175 (31%)	6 (38%)	181 (31%)
Total	561 (100%)	16 (100%)	577 (100%)

^aSee *Methods* for the description of how these were determined.

^bIncludes both locations in which a peak was only present upstream of the gene of interest (217 for α ; 300 for α), as well as those in which peaks flanked the gene of interest (63 for α ; 74 for α).

^cIncludes locations in which a peak was observed downstream of the gene of interest.

regulated genes were grouped as “Intergenic” peaks, and these designations were used in [Supplementary Figure S3A and Table S8](#). Some of the “UTR/ORF” peaks in [Supplementary Figure S3A](#) had Tup1 occupancy that spanned intergenic and UTR sequences upstream of a possible target gene. For [Table 2](#) analysis, these peaks were classified as “Upstream,” based upon examination in the IGV genome browser (Broad Institute).

Results

Genetic screens identified several Tup1 WD domain mutants that increase *HO* expression

Having identified a *tup1* mutation as a suppressor of *HO* transcription in the absence of the Swi5 transcription factor ([Parnell and Stillman 2019](#)), we next sought to identify additional residues of Tup1 that participate in repression of the *HO* promoter by conducting two targeted genetic screens. Each screen was performed using a yeast strain in which *HO* expression was decreased due to the absence of an activator or coactivator of the *HO* promoter. Strains carried an *HO-ADE2* reporter, allowing the level of *HO* expression to be observed as growth on media lacking adenine ([Jansen et al. 1996](#)). The chromosomal copy of *TUP1* was deleted and covered with a *TUP1*-containing plasmid. We then swapped this with a PCR-mutagenized version of *TUP1* and isolated alleles that elevated *HO-ADE2* expression, as determined by increased growth on -Ade media.

The first screen with the mutagenized *TUP1* gene was conducted in a *swi5 ash1* strain similar to that used to identify the *tup1(H575Y)* allele ([Parnell and Stillman 2019](#)). Swi5 is the pioneer activator of *HO* expression; its binding to two sites within the promoter sets in motion a series of factor recruitments, histone-modifications, and nucleosome evictions that ultimately allow activation of transcription ([Cosma et al. 1999](#); [Bhoite et al. 2001](#); [Takahata et al. 2009](#); [Stillman 2013](#)). Expression of *HO-ADE2* in a *swi5* mutant is extremely low, and cells grow very poorly in absence of adenine ([Parnell and Stillman 2019](#)). Ash1 is a repressor of *HO* expression that acts predominantly in daughter cells, leading to expression of *HO* only in mother cells ([Bobola et al. 1996](#); [Sil and Herskowitz 1996](#)). We previously determined that additional negative regulators of *HO* could be detected using the *HO-ADE2* reporter, but only when an *ash1* mutation was added to the *swi5* strain. This increased the baseline expression of the *HO* promoter enough to allow loss of another repressor to be visible as increased growth on media lacking adenine ([Parnell and Stillman](#)

[2019](#)). Several negative transcription factors participate in *HO* regulation, and substantial increases in expression were only observed upon removal of multiple of these factors simultaneously ([Parnell and Stillman 2019](#)).

While the screen conducted in a *swi5 ash1* strain was productive for isolating the *tup1(H575Y)* mutant allele, the later discovery that Ash1 is responsible for most of the Tup1 recruitment to the *HO* promoter suggests an *ASH1* strain could be better suited for identification of *tup1* alleles ([Parnell et al. 2020](#)). Therefore, we conducted a second screen involving a mutagenized *TUP1* plasmid in a *gcn5* mutant background. Gcn5 is the catalytic subunit of a histone acetyltransferase complex required for full *HO* expression ([Cosma et al. 1999](#); [Takahata et al. 2011](#)). In the absence of Gcn5, *HO-ADE2* expression decreases to a level similar to that of an *swi5 ash1* strain, providing a baseline level of growth on -Ade media that allowed small increases in *HO-ADE2* expression to be visible as more robust growth ([Parnell and Stillman 2019](#)).

Mutants of Tup1 identified in the two screens are listed in [Table 1](#). The apparent bias toward mutations identified in the *swi5 ash1* screen reflects different validation procedures used for the screens rather than a difference in the sensitivity of the screens (see *Methods* for additional explanation). While the entire *TUP1* gene was PCR-mutagenized, all mutants from the two screens fell within the WD domain of the protein, known to interact with the $\alpha 2$ repressor and suggested to participate in multiple types of protein–protein interactions with other DNA-binding proteins ([Komachi et al. 1994](#); [Carrico and Zitomer 1998](#)).

Most mutations were located within WD repeats 4–7, including multiple hits at position H575, which was the site of the originally isolated *tup1(H575Y)* allele ([Table 1](#), [Figure 1, A and B](#)). Several mutations were also identified within the DA loops between successive WD repeats ([Table 1](#); Y445, E526, N569, E570, H575, H629, and N673). Of these residues, Y445, E526, and N673 are exposed on the top surface of the WD domain ([Figure 1B](#)). Y445 and N673 were previously identified as contact points with the $\alpha 2$ repressor ([Komachi et al. 1994](#)).

Multiple sites affected by the mutations are likely important for the stability of their respective WD repeats. Within each repeat, interactions among a structural tetrad of amino acids are important for maintaining stability; these include the tryptophan in the C sheet, the serine/threonine in the B sheet, the histidine in the DA loop, and the aspartic acid in the tight BC turn ([Sprague et al. 2000](#)). Our screens identified mutations in S649, H575, H629, D597, and D699, all of which are residues thought to participate

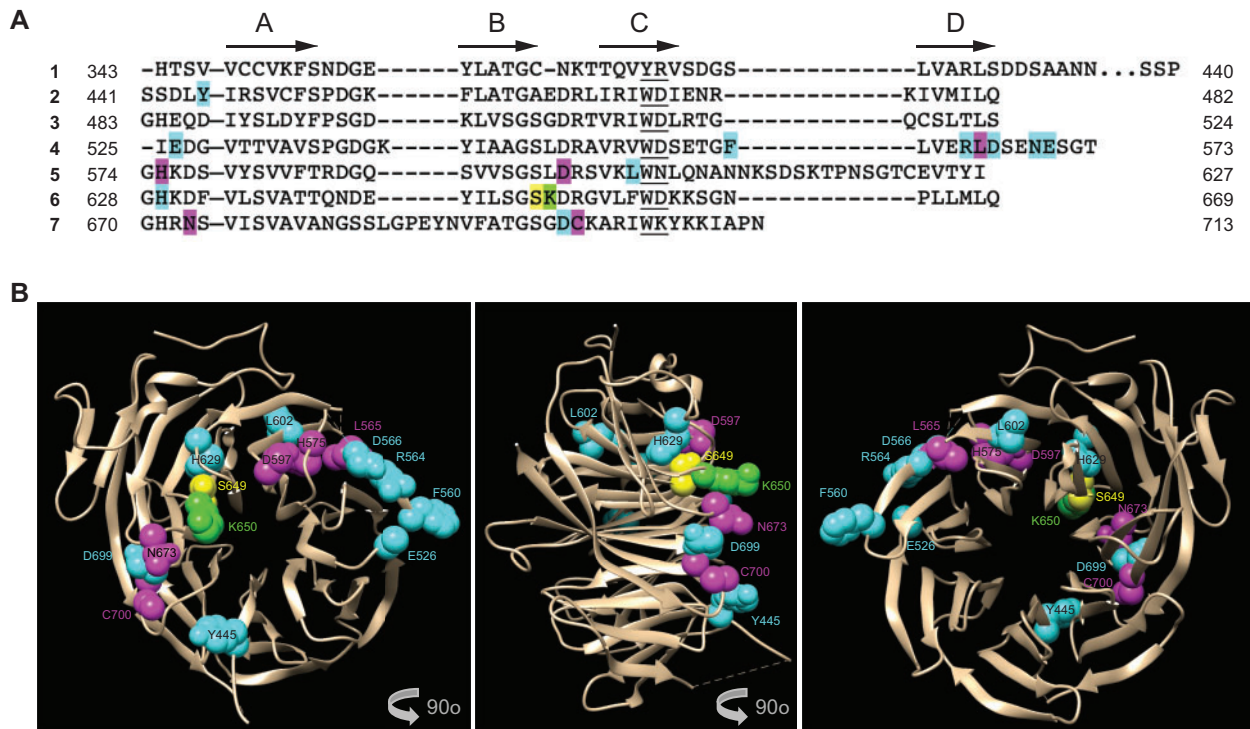


Figure 1 Tup1 mutants identified in genetic screens for activation of *HO* expression. (A) All *tup1* mutations were located with the WD domain at the C-terminus of Tup1. The amino acid sequence of the WD domain of Tup1 is shown, with each line representing the WD repeat number on the left. Amino acid number positions are indicated. Beta sheets determined in Sprague et al. (2000) are indicated by arrows and the A–D designation above the sequence. Forty-eight amino acids from the DA loop between WD repeats 1 and 2 were eliminated for simplicity (H390 to S437), as indicated by “...” The WD or variant motif within each repeat is underlined. Highlighted amino acids represent mutation positions: yellow for S649, green for K650, magenta for the other five mutants for which endogenous mutants were constructed and tested for effects on *HO* expression (L565, D597, N673, and C700), and teal for all other mutants listed in Table 1. (B) Most mutations lie on one surface of the propeller. The structure of the WD domain of Tup1 (Sprague et al. 2000) is shown, with mutant positions indicated. Color coding is the same as in (A). Note that mutants at positions N569 and E570 are not shown because they were not in the resolved structure. The central image is a 90° rotation relative to the left image, to show the amino acids, including K650, that project from the surface of Tup1, and the right image is another 90° rotation to illustrate the opposite surface.

in these structural interactions. The aspartic acid within this structural tetrad is the most invariant amino acid position across WD repeats in different proteins, and two of our mutations are at these locations (D597 and D699; Sprague et al. 2000). The importance of these positions is also highlighted by the observation that mutations in positions H575, H629, and D699 were identified in both screens.

The *tup1*(S649F) mutant displays an α cell-predominant slow growth phenotype

We chose a panel of six mutations for further study, representing the most frequently mutated amino acids and a variety of positions within the WD domain (Table 1, indicated in red). These include the original *tup1*(H575Y) allele as well as *tup1*(L565P), *tup1*(D597N), *tup1*(S649F), *tup1*(N673D), and *tup1*(C700R). Strains were constructed with each of these mutations at the endogenous, unmarked *TUP1* locus and then assessed for phenotypes resembling those of *tup1* null mutants.

Strains that are *tup1* null grow poorly and experience a delay in G1 of the cell cycle. Of the *tup1* point mutants we examined, only *tup1*(S649F) showed an obvious slow growth phenotype at the three temperatures examined (Figure 2A). While the effect was subtle in the *tup1*(S649F) MAT α strain, there was a more obvious growth defect at all temperatures in the MAT α strain. A W303 strain with the *TUP1* gene deleted shows a growth defect that is more severe than for *tup1*(S649F) (Figure 2B). Additionally,

Anchor Away depletion of Tup1 in W303 causes a transient G1 arrest (Parnell and Stillman 2019). Thus, *tup1*(S649F) is distinct from the null allele.

MAT α *tup1* strains show decreased mating to α strains, increased mating to α strains, and a “shmoo”-like phenotype reminiscent of α cells that are responding to α -factor, resulting from misregulation of mating-type-specific genes normally repressed by Tup1 (Wickner 1974; Lemontt et al. 1980; Mukai et al. 1991). The *tup1*(S649F) α cells also had a shmoo-like appearance and experienced a delay in mating but later was capable of mating with both α and α *TUP1* strains (data not shown). Other *tup1* point mutants did not display mating irregularities (data not shown).

Cells lacking *TUP1* are also flocculent, due to inappropriate expression of the agglutinin genes, a class of cell surface glycoproteins repressed by Tup1 (Lipke and Hull-Pillsbury 1984). Most *tup1* mutant alleles had only minor flocculation phenotypes (data not shown). However, both α and α *tup1*(S649F) strains displayed a strong flocculation phenotype, with the effect in the α strain more severe than in the α strain, approaching the level of flocculation of a *tup1* null. Collectively, the reduced growth, mating characteristics, and flocculation phenotype of *tup1*(S649F) suggest this mutant substantially diminishes but does not eliminate Tup1 function, as its properties are similar to but not as severe as a *tup1* null. The slow growth and flocculation phenotypes of *tup1*(S649F) are lost in a heterozygous diploid, demonstrating that this allele is recessive for these characteristics.

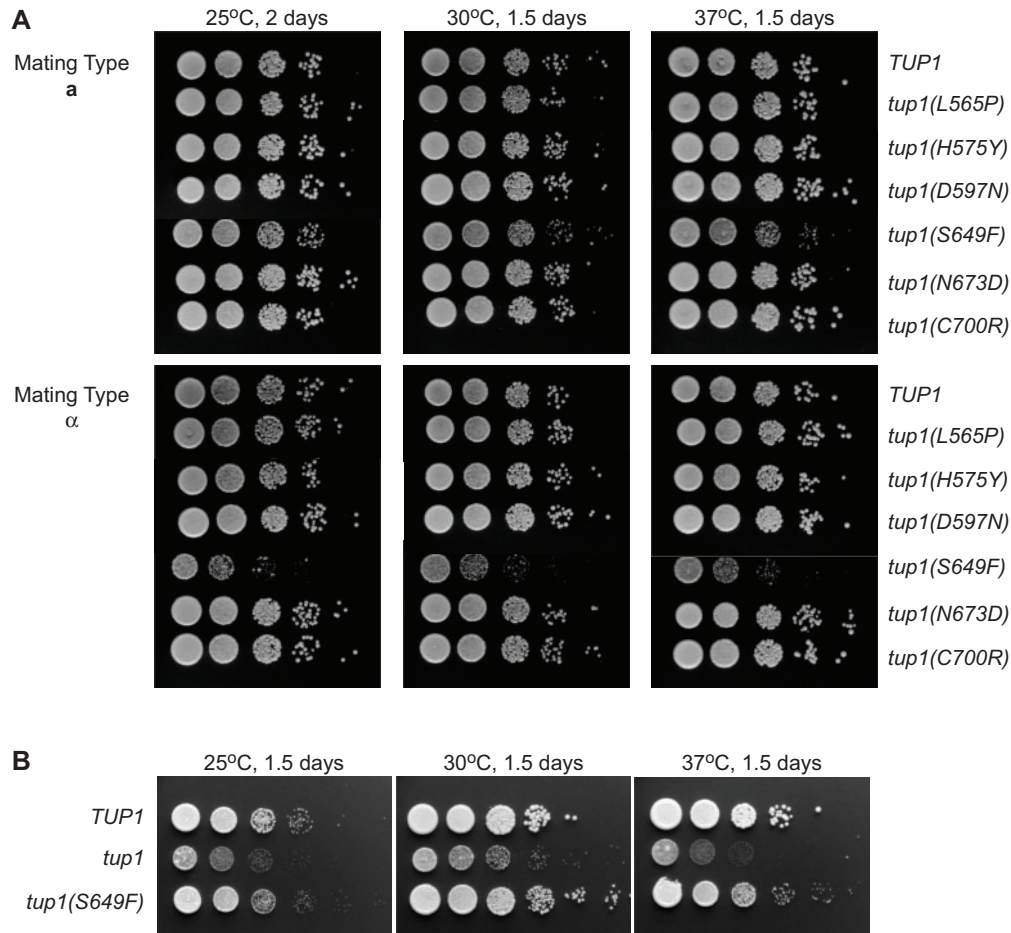


Figure 2 The *tup1(S649F)* mutant shows a growth defect that is stronger in the α strain. Shown are 10-fold serial dilutions of the *tup1* mutants indicated at the right, compared to *TUP1* wild type, grown on YPAD media at the indicated temperatures and time durations. (A) Comparison of *tup1* point mutants obtained in genetic screens. Strains with mating type **a** are on top; strains with mating type α are on the bottom. (B) Comparison of *tup1(S649F)* with a *tup1* null in the MAT**a** background.

The *tup1(S649F)* mutant allows substantial increases in *HO* expression

To assess the effects of the *tup1* point mutants on native *HO* expression rather than the *HO-ADE2* reporter used for our screens, we measured the level of endogenous *HO* expression in *tup1* mutants by RT-qPCR within the context of an *swi5 ash1* strain, a *gcn5* strain, and an otherwise wild-type strain (Figure 3, A–C). All *tup1* mutations increased expression of *HO* in the *swi5 ash1* strain, even the *tup1(S649F)* mutation isolated only from the *gcn5* screen (Figure 3A). The *tup1(S649F)* and *tup1(N673D)* mutations increased expression most strongly, more than threefold over the level of *HO* expression in the *swi5 ash1* strain. All mutations also increased *HO* expression in a *gcn5* strain with a significance level of $P < 0.05$, but most of these increases were less than twofold (Figure 3B). The exceptions were *tup1(D597N)* (just over twofold increase) and *tup1(S649F)*, identified originally only in the *gcn5* screen (nearly sevenfold increased expression). Within the context of an otherwise wild-type strain, most mutations increased *HO* expression only very modestly (Figure 3C). The *tup1(S649F)* mutation, however, displayed a greater than twofold increase in expression.

Our genetic screens were therefore effective in identifying additional *tup1* mutations at a variety of positions in the WD domain that suppress *swi5 ash1* and *gcn5* for expression of *HO* and likely affect the regulation of additional *Tup1* target genes. The

strongest of these was *tup1(S649F)*, as measured by its effect on growth, mating, flocculation, and *HO* expression both alone and via suppression of *swi5 ash1* and *gcn5* mutants. The S649 amino acid has been predicted to contribute to the structural stability of the 6th WD repeat via a tetrad of interactions between H629, S649, D651, and W657 (Sprague 2000). Loss of integrity of this repeat could destabilize the WD domain and possibly the entire protein. To examine this possibility, we tagged wild-type *Tup1* and *Tup1(S649F)* with a V5 epitope tag and visualized protein expression and stability by western blot (Supplementary Fig. S1). As predicted, the protein level of *Tup1(S649F)* was reduced relative to wild type. Effects of the *tup1(S649F)* mutation could therefore largely result from a diminished level of stable protein. Importantly, however, the phenotype of the *tup1(S649F)* mutant is less severe than a *tup1* null mutant (Figure 2B).

Effects of *tup1(S649F)* on *HO* transcription are not caused by a loss of post-translational modifications

An alternative possibility for the effects of the *tup1(S649F)* mutation on growth and *HO* expression could be a loss of post-translational modification of *Tup1* via one of two mechanisms. Serine 649 could be modified by phosphorylation, or the immediately adjacent amino acid, a lysine residue at position 650, could be acetylated. Residue K650 appears to project outward from one

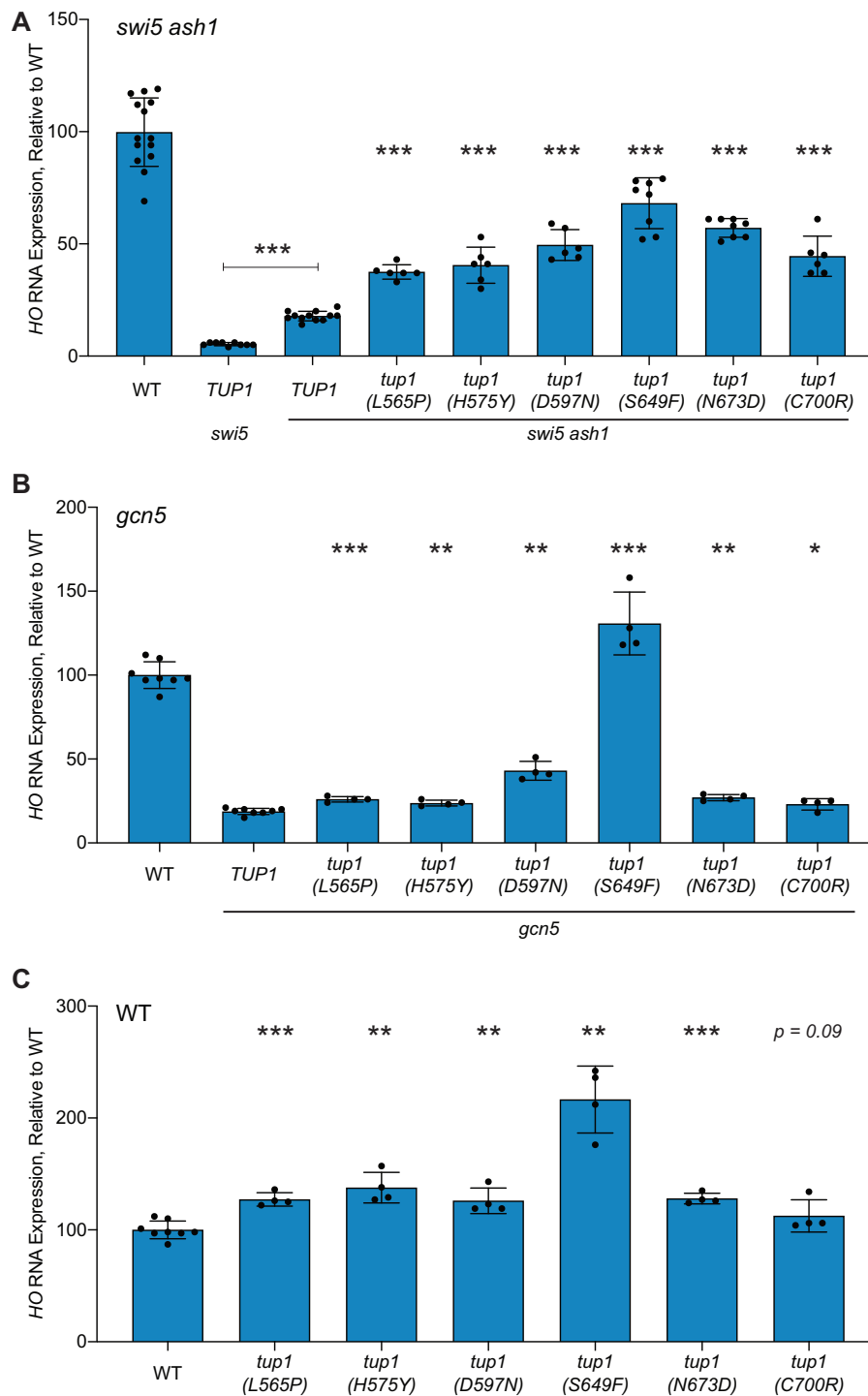


Figure 3 HO expression increases substantially in the *tup1*(S649F) mutant. HO mRNA levels were measured by RT-qPCR, normalized to RPR1, and expressed relative to wild type. Each dot represents a single data point, and error bars reflect the standard deviation. *** $P < 0.001$, ** $P < 0.01$, * $P < 0.05$. (A) Mutant *tup1* alleles increase HO expression in an *swi5 ash1* strain. Asterisks above each *tup1* point mutant denote the P-value comparison of the indicated *swi5 ash1 tup1* strain relative to the *swi5 ash1 TUP1* strain. (B) The *tup1*(S649F) mutant displays strong suppression of a *gcn5* mutant at the HO gene. Asterisks above each *tup1* point mutant denote the P-value comparison of the indicated *gcn5 tup1* strain relative to the *gcn5 TUP1* strain. (C) The *tup1*(S649F) mutant increases HO expression in an otherwise wild-type context. Asterisks above each *tup1* point mutant denote the P-value comparison of the indicated *tup1* strain relative to the *TUP1* wild-type strain.

surface of the WD domain, and S649 is positioned just beneath it (Figure 1B), suggesting that the effect of *tup1*(S649F) may be the introduction of a bulky amino acid that would alter the positioning of K650, impairing the ability to be acetylated or deacetylated. There is precedent in the literature for the regulation of chromatin and transcriptional-related proteins by acetylation (Narita

et al. 2019). One of these methods of post-translational modification could provide a mechanism for switching between active and repressive forms of Tup1, consistent with the model in which Tup1 masks activation domains but subsequently participates in gene activation. We tested these possibilities by constructing additional mutants at positions 649 and 650 and measuring

suppression of *HO* expression in *swi5 ash1* and *gcn5* strains relative to the original *tup1(S649F)* mutant.

A *tup1(S649A)* mutant was used to test the possibility that an inability to phosphorylate S649 is the critical reason for the effect of *tup1(S649F)* on *HO* expression. The *tup1(S649A)* mutation, in sharp contrast to *tup1(S649F)*, had no effect on *HO* expression in either a *swi5 ash1* or a *gcn5* strain (Figure 4, A and B). This result

demonstrates that the introduction of the phenylalanine amino acid, rather than a simple loss of possible S649 phosphorylation by substitution of a different amino acid, is important for the observed *tup1(S649F)* phenotype.

Two mutations, *tup1(K650Q)* and *tup1(K650R)*, were constructed to mimic either permanent acetylation or deacetylation of K650, respectively. Interestingly, the *tup1(K650Q)* mutant

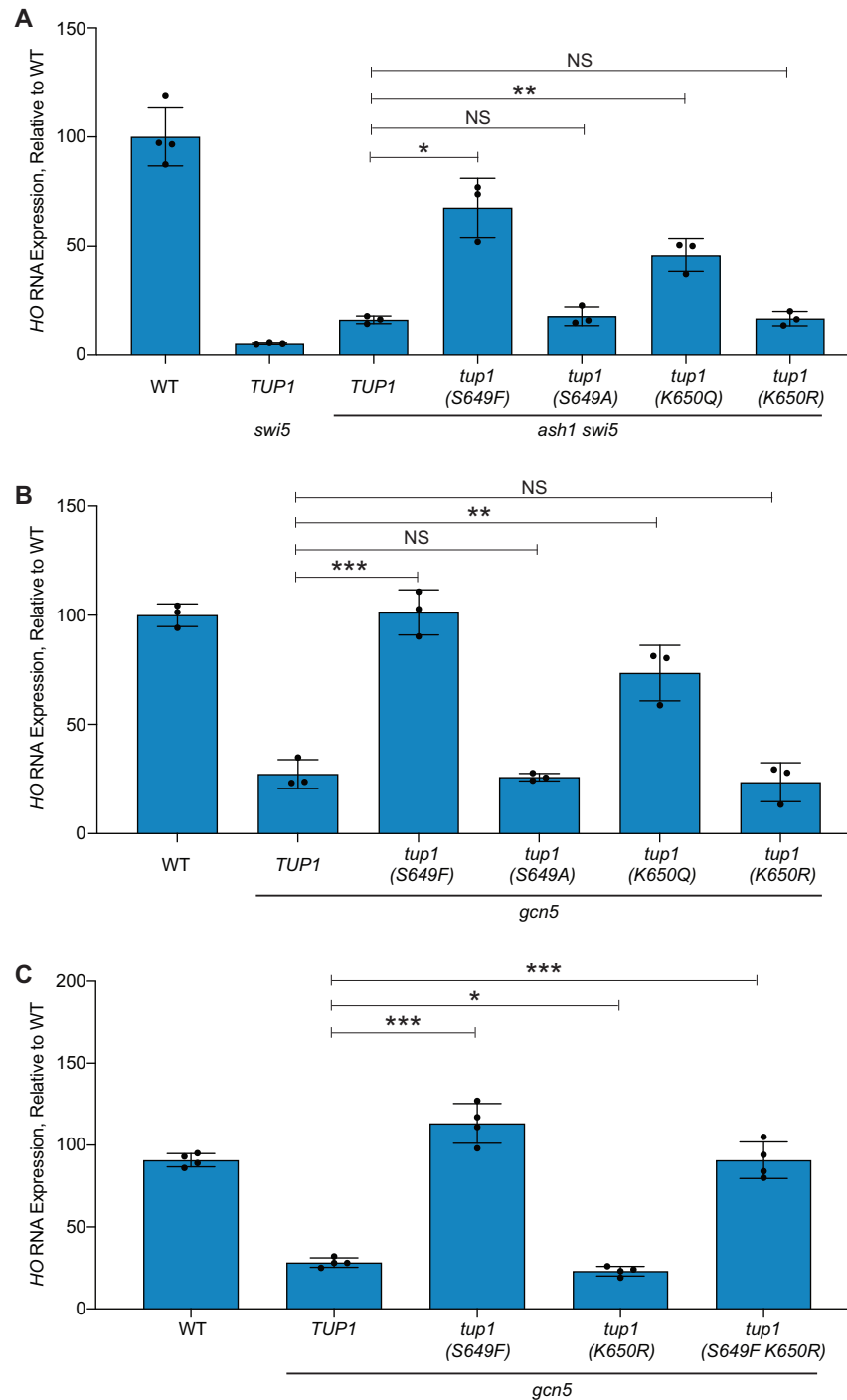


Figure 4 The transcriptional effects of *tup1(S649F)* are not due to changes in post-translational modifications. *HO* mRNA levels were measured by RT-qPCR, normalized to *RPR1*, and expressed relative to wild type. Each dot represents a single data point, and error bars reflect the standard deviation. *** $P < 0.001$, ** $P < 0.01$, * $P < 0.05$, NS = not significant. (A) The *tup1(S649F)* and *tup1(K650Q)* mutants increase *HO* expression in a *swi5 ash1* strain, while *tup1(S649A)* and *tup1(K650R)* fail to do so. (B) Suppression of *gcn5* is specific to the *tup1(S649F)* and *tup1(K650Q)* alleles. (C) The *tup1(S649F K650R)* double mutant retains the *gcn5* suppression exhibited by the *tup1(S649F)* single mutant.

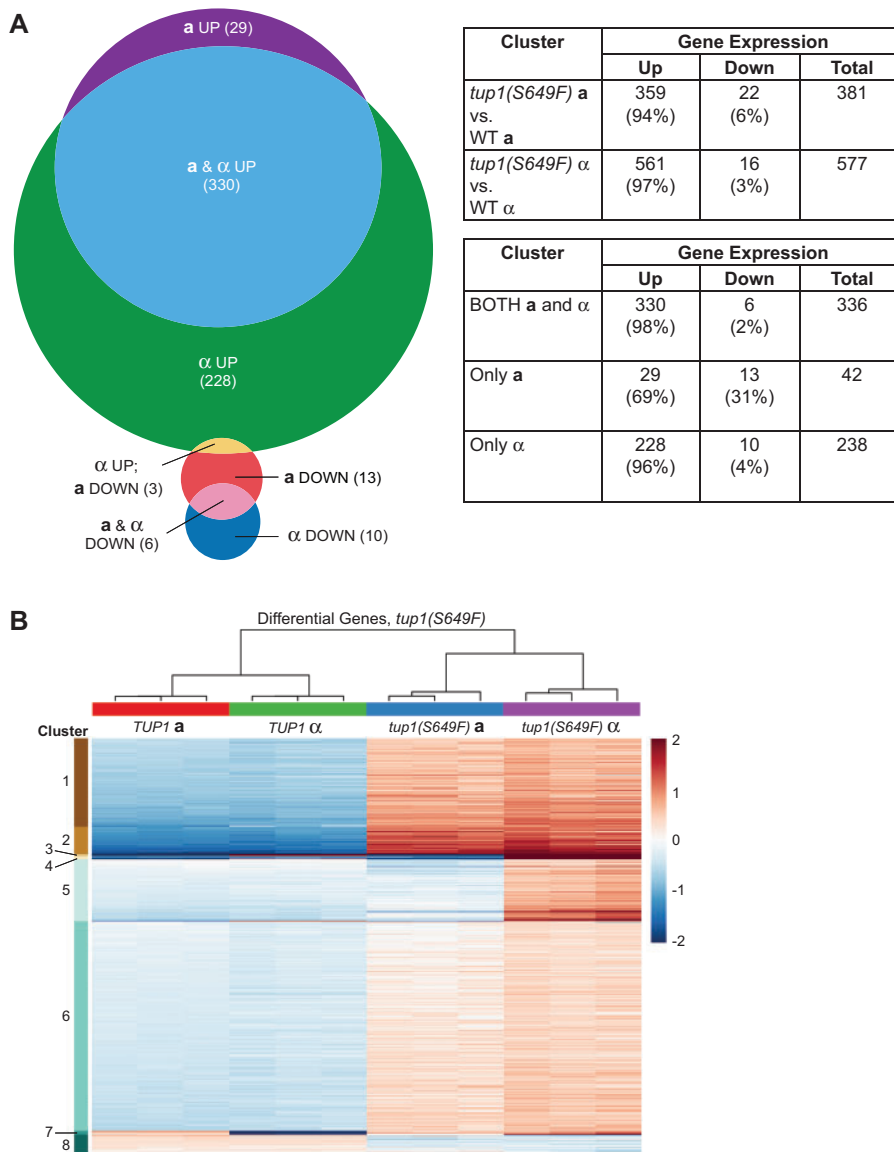


Figure 5 The *tup1(S649F)* mutant affects expression of many genes. (A) A large number of genes show altered expression in both mating types of the *tup1(S649F)* mutant. Protein-coding genes for which RNA-Seq showed a greater than twofold increase (“Up”) or decrease (“Down”) in expression were counted for each comparison of *tup1(S649F)* to wild type (WT) in each mating type. Percentages indicate the proportion of increased or decreased genes out of each horizontal total. The top table shows the number of genes with altered expression in each mating type. The bottom table indicates the number of these genes that exhibited an expression change in both mating types (“Both a and alpha”) vs those that were mating-type specific (“a Only” or “alpha Only”). Overlap is shown visually in the Venn diagram at the left. Three genes were not counted in “Both” or “a/alpha Only” due to increased expression in one mating type and decreased expression in the other mating type. (B) k-means clustering highlights different groups of genes altered in the *tup1(S649F)* mutant. The heat map depicts RNA expression levels among the different genotypes listed at the top, expressed as mean-centered relative log values, with each row representing an individual gene. Triplicate biological samples for each genotype are shown as individual columns. Only genes that displayed a greater than twofold difference in at least one comparison between mutant and wild type and between a and alpha cells are displayed (642 total). Genes were sorted by an unsupervised k-means clustering algorithm into eight clusters. The hierarchical tree above the heat map indicates the degree of relationship between samples, and the color scale at the right indicates the level of \log_2 -fold enrichment.

displayed suppression of *HO* expression in the *swi5 ash1* and *gcn5* strains, albeit at a lower level than *tup1(S649F)*, while the *tup1(K650R)* mutant had no effect (Figure 4, A and B). The difference in expression effects upon substitution of lysine with glutamine or arginine suggests the possibility that acetylation of K650 could play a role in Tup1 regulation. If acetylation of Tup1 were necessary to “turn off” its repressive capacity, then a glutamine permanent acetylation mimic (Q) would be expected to be a weaker repressor. *HO* expression would then increase specifically in the *tup1(K650Q)* mutant, as observed. An arginine permanent deacetylation mimic (R) should not have the same effect.

One hypothesis for the transcriptional effects of *tup1(S649F)* is that it may position K650 such that it can be acetylated but not deacetylated. Tup1 would thus become locked in a “repressor off” state, explaining the similarity between the *tup1(S649F)* and *tup1(K650Q)* mutants. If this scenario explains the phenotype of *tup1(S649F)*, then combination of *tup1(S649F)* with *tup1(K650R)*, which cannot be acetylated, should not allow the increases in *HO* transcription observed in the *tup1(K650Q)* mutant. However, a *tup1(S649F K650R)* double mutant still displayed suppression of a *gcn5* mutant for *HO* expression, suggesting the addition of the bulky phenylalanine group at position 649 has a different effect

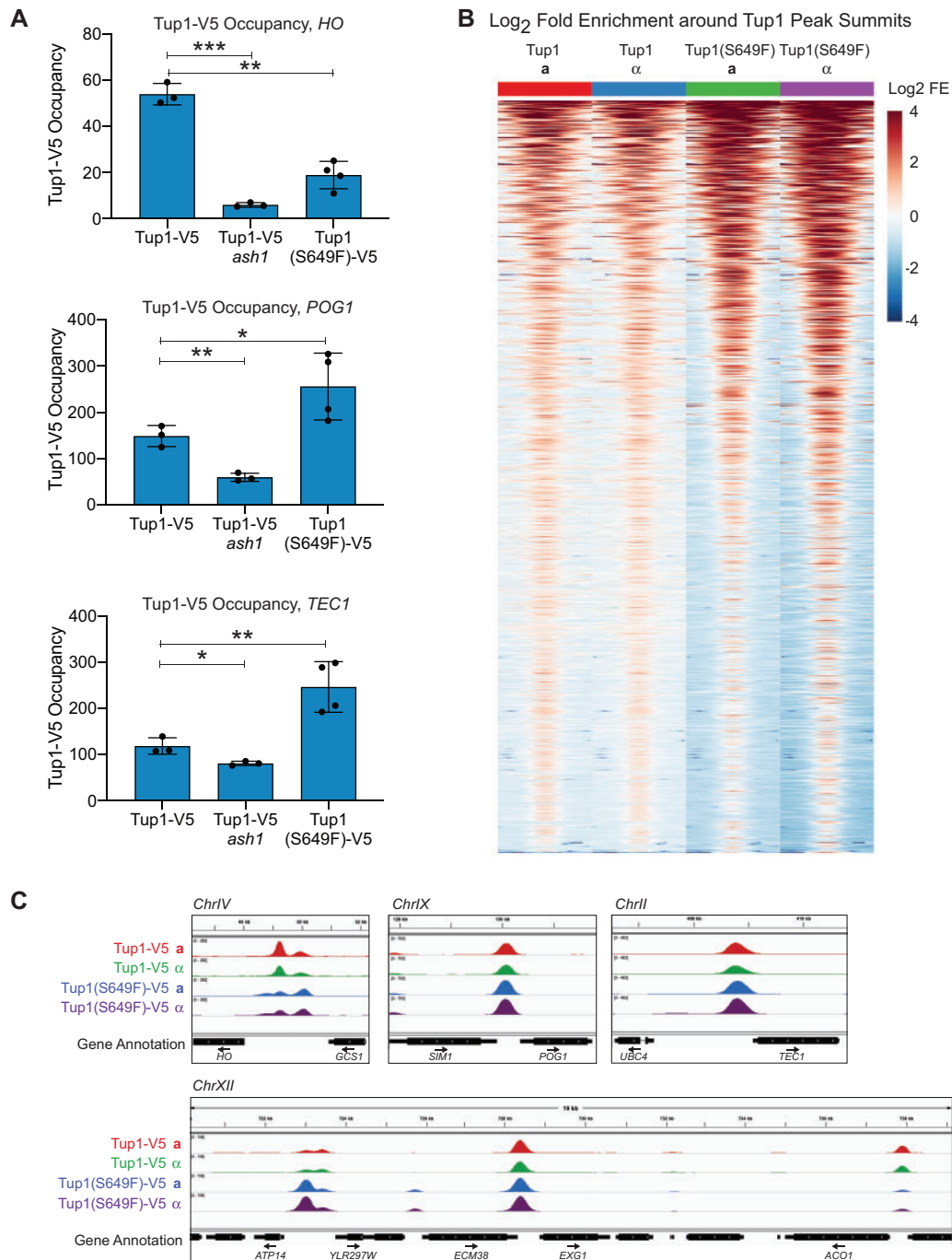


Figure 6 The *tup1(S649F)* mutant displays increased occupancy relative to wild type at many genomic locations. (A) Tup1(S649F) occupancy decreased at the *HO* promoter but increased at the intergenic regions upstream of *POG1* and *TEC1*. Tup1-V5 ChIP analysis, showing enrichment upstream of the *HO* (−1295 to −1121), *POG1* (−570 to −435), and *TEC1* (−433 to −259) genes. For each sample, occupancy was normalized to its corresponding input DNA and to a No Tag control. Each dot represents a single data point, and error bars reflect the standard deviation. ****P* < 0.001, ***P* < 0.01, **P* < 0.05. (B) Occupancy of Tup1(S649F) appears to be higher than wild-type Tup1 occupancy at most genomic locations. Heat maps depict the log₂-fold enrichment of Tup1-V5 and Tup1(S649F)-V5 at peak summits genome-wide (1266 peaks), displaying enrichment from −625 to +625 relative to the center of each Tup1-V5 peak, in bins of 25-bp. The data for each strain represent an average of three biological replicates, and the color scale at the right indicates the level of log₂-fold enrichment. Each horizontal line depicts a single Tup1-V5 peak. (C) Tup1(S649F) occupancy shows variation among individual genomic sites. Snapshots of ChIP-Seq results from the Genome Browser IGV (Broad Institute) show the sequenced fragment pileups for the intergenic regions upstream of *HO* (Top Left), *POG1* (Top Middle), and *TEC1* (Top Right), and a region of chromosome XII (Bottom). The colored tracks show ChIP-Seq results for Tup1-V5 WT **a** (red), Tup1-V5 WT α (green), Tup1(S649F)-V5 **a** (blue), and Tup1(S649F)-V5 α (purple). The bottom track displays gene annotations. The four samples were group autoscaled independently at each location, to account for differences in enrichment between sites. Tracks represent an average of three biological replicates.

(Figure 4C). A change in acetylation state is, therefore, unlikely to explain the transcriptional effects of the *tup1(S649F)* and *tup1(K650Q)* mutants. A more plausible explanation, as suggested

above, is that mutation of S649F diminishes Tup1 protein stability by disrupting the 6th WD repeat, reducing the amount of Tup1 available for affecting gene expression. Alternatively, or in

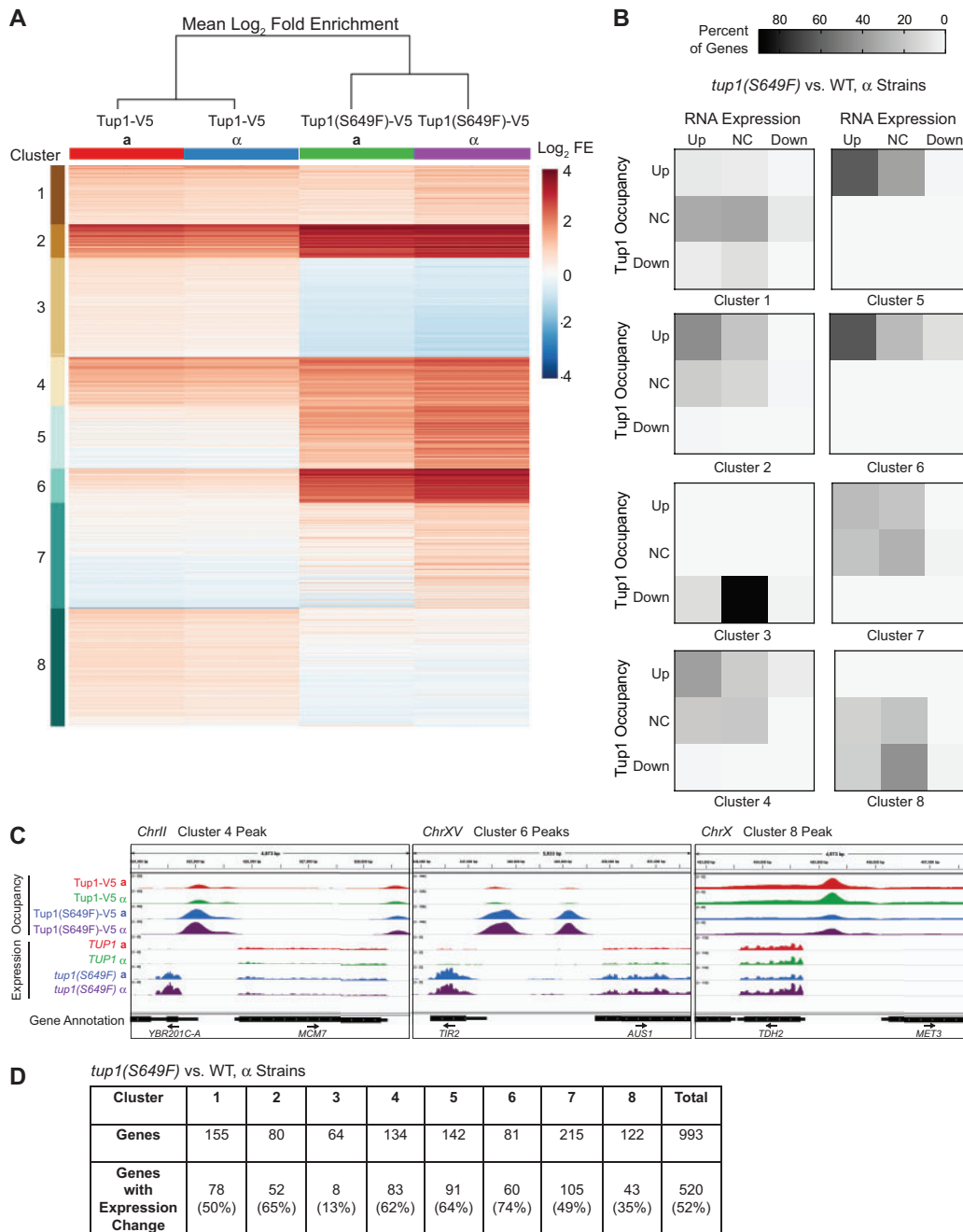


Figure 7 Gene expression changes tend to occur at Tup1 intergenic sites with increased Tup1(S649F) occupancy. (A) Groups of Tup1 peaks show differences in Tup1 vs Tup1(S649F) occupancy. The heat map depicts the mean Tup1 log₂-fold enrichment among the different genotypes listed at the top (each an average of triplicate biological samples). The rows represent sites of Tup1 occupancy (1266 total). Tup1 peaks were sorted by an unsupervised k-means clustering algorithm into eight clusters. The hierarchical tree above the heat map indicates the degree of relationship between samples. (B) Increased Tup1-S649F occupancy often occurs in conjunction with increased the expression of downstream genes. Each square within the 3 × 3 heat maps represents a unique combination of Tup1 occupancy and RNA expression of the downstream gene, where “Up” and “Down” indicate increased or decreased occupancy/expression in *tup1(S649F)* α vs wild-type α, respectively, and “NC” (No Change) indicates less than 1.5-fold alteration in levels. The color scale at the top indicates the percentage of genes in each category. Genes were separated by cluster from (A) and were only included if they were located downstream of a Tup1 peak and had a valid expression level from RNA-Seq (993 total). Peaks were counted twice if present between divergent genes. Some genes were counted more than once, due to two or three Tup1 peaks within the intergenic region upstream of the gene (53 total). (C) Individual Tup1 occupancy sites show different effects on the expression of downstream genes. Snapshots of ChIP-Seq (Occupancy) and RNA-Seq (Expression) results from the Genome Browser IGV (Broad Institute) show the sequenced fragment pileups for representative peaks on chromosomes II, XV, and V (examples from clusters 4, 6, and 8). Tracks represent an average of three biological samples for each strain. The four strains for each experiment were autoscaled as a group for occupancy and expression separately to account for differences in fragment depth between locations. Colors for both ChIP-Seq and RNA-Seq are as follows: Tup1-V5 WT a (red), Tup1-V5 WT α (green), Tup1(S649F)-V5 a (blue), and Tup1(S649F)-V5 α (purple). The bottom track displays gene annotations. Gene names are indicated for those located downstream of a Tup1 peak. (D) Approximately half of the genes downstream of Tup1 peaks show altered expression in the *tup1(S649F)* α mutant. Shown are the number and percentage of genes downstream of Tup1 peaks in each cluster from (A) with >1.5-fold change in RNA-Seq values between *tup1(S649F)* α and wild-type α.

addition, the S649F substitution could affect Tup1 interaction with other proteins.

Many genes are upregulated in *tup1(S649F)*, both in **a** and **α** strains

The diminished Tup1(S649F) protein level relative to wild type suggests this mutant is a hypomorph, expected to display similar but reduced phenotypes and transcriptional changes as a *tup1* null mutant. The slow growth, mating, and flocculation phenotypes of *tup1(S649F)* strains fit this prediction. The difference in growth phenotype between **a** and **α** *tup1(S649F)* mutants has not, to our knowledge, been noted in *tup1* null mutants and suggests expression of Tup1-regulated genes in *tup1(S649F)* may not be identical to that of a *tup1* null. To investigate the nature of transcriptional changes in the *tup1(S649F)* mutants, we performed RNA-Seq analysis, comparing genome-wide expression in wild-type and *tup1(S649F)* strains of both mating types (Supplementary Table S3). Strains that were *tup1* null were not included in our RNA-Seq analysis, as frequent development of suppressors in the W303 *tup1* strain led to inconsistencies in expression results between biological samples (Figure 2B; data not shown).

As expected for the impaired function of a corepressor protein, both *tup1(S649F)* mating types displayed upregulation of a large number of genes (Figure 5A, Supplementary Table S4). The **α** strain had more changes than the **a** strain (561 vs 359 upregulated genes). Only a small minority of genes in both mating types were downregulated (<10% of the total changed genes), fewer than have been previously observed in a comparison of a *tup1* null with wild type (Chen et al. 2013), conducted in S228c strains.

A heat map showing relative expression values for all differentially expressed genes ($P < 0.05$) that exhibited a greater than two-fold increase or decrease between mutant and wild type is shown in Figure 5B. The genes were organized into clusters by a k-means algorithm, using eight clusters to emphasize the pattern of gene expression changes between strains. Clustering showed groups of genes with increased expression in both mating types in the *tup1(S649F)* mutant strains (Clusters 1, 2, and 6) as well as one group with decreased expression (Cluster 8). Cluster 5 highlighted genes for which expression increased only in the **α** mating type of the mutant strain. The small number of genes that were differentially expressed in **a** vs **α** strains, either in wild type or mutant or both, comprised Clusters 3, 4, and 7 (discussed below). A comprehensive list of all genes with greater than a twofold change in expression in mutant vs wild type for both mating types is provided in Supplementary Table S4.

Gene ontology (GO) analysis identified several categories of genes that displayed increased expression in *tup1(S649F)* in each mating type (Supplementary Table S5). Consistent with previous reports, these included genes involved in carbohydrate metabolism, oxidation/reduction, transmembrane transport, and cell wall organization (Derisi et al. 1997; Green and Johnson 2004). In addition, the transcription of some DNA-binding transcription factors was altered. A large number of genes that were altered in the *tup1(S649F)* mutant encoded proteins found at the cell periphery. Genes shown previously to be regulated by Tup1 via different repressor proteins were found to be upregulated, including **a**-specific MFA2, glucose-repressed SUC2, oxygen-repressed ANB1, HEM13, and DAN1, glucose-regulated HXT genes, DNA damage response genes RNR2, 3, 4, and flocculation FLO genes. The effect of *tup1(S649F)* on these diverse pathways suggests a general loss of repression by the mutant protein. All of the same categories of genes were identified when comparing *tup1(S649F)* **α** expression

to wild-type **α** expression. However, mutant **α** strains exhibited additional changes in genes involved in small molecule and organic acid metabolic processes, cellular response to chemical stimuli, and sexual reproduction (Supplementary Table S5). As suspected from the differential growth phenotype in *tup1(S649F)* **a** and **α** cells relative to *tup1* null, many changes in the *tup1(S649F)* **α** strain relative to wild type were not identified in a previous comparison of *tup1* null and wild-type **α** strains (discussed further below; Chen et al. 2013). Performing GO analysis on individual k-means clusters from Figure 5B failed to identify additional categories of genes regulated by Tup1 or to demonstrate that particular clusters contained a high percentage of genes with similar functions.

Tup1(S649F) shows increased association at many genomic locations

The reduced level of Tup1(S649F) protein relative to wild type, particularly in the **α** strain (Supplementary Figure S1), suggests the transcriptional effects of *tup1(S649F)* could be due to less Tup1 protein bound within target promoter regions. General loss of Tup1 protein across the genome could explain the observed upregulation of Tup1 target genes controlled by different repressors and would suggest *tup1(S649F)* largely behaves as a hypomorph. This is supported by the observation that the *tup1(S649F)* mutation reduced but did not eliminate Tup1 occupancy in a ChIP assay to its most predominant site in the *HO* promoter (Figure 6A, Top). However, the association of Tup1(S649F) with two other target promoters, POG1 and TEC1, was increased relative to wild type (Figure 6A, Middle and Bottom). The increased occupancy of Tup1(S649F) is difficult to reconcile with the observations of a reduced level of protein relative to wild type and the upregulation of many genes. We, therefore, performed ChIP-Seq to investigate the association of Tup1 and Tup1(S649F) with their genome-wide targets in both **a** and **α** mating types.

Distinct differences were observed between ChIP-Seq samples of Tup1 wild-type and Tup1(S649F) of both mating types conducted with triplicate biological samples, as judged by Pearson correlation (Supplementary Figure S2). In contrast to the expectation that Tup1 occupancy would be reduced in the Tup1(S649F) mutant, we observed an overall stronger association of the mutant Tup1 protein with chromatin than wild-type Tup1, visualized by higher \log_2 fold enrichment at peaks across the genome (Figure 6B). This suggests that the POG1 and TEC1 upstream regions tested are reflective of the genome-wide changes in Tup1 occupancy in the *tup1(S649F)* mutant. At the *HO* promoter, ChIP-Seq showed that while the major peak of Tup1 occupancy at *HO* was reduced in *tup1(S649F)*, as we had observed in the qPCR analysis (Figure 6A), the minor peak of Tup1 occupancy at *HO* actually increased in the mutant strain, similar to those within the POG1 and TEC1 upstream regions (Figure 6C, ChrIV).

Visualization of ChIP-Seq fragment densities across the genome with the IGV genome browser (Broad Institute) suggested that Tup1 occupancy was redistributed in the *tup1(S649F)* mutant relative to wild type. While many locations displayed increased occupancy in the mutant relative to wild type, some appeared mostly unaltered, and some had decreased occupancy (Figure 6C). New peaks seemed to appear in the mutant, but careful observation in a genome browser showed that these locations had a small amount of Tup1 occupancy in wild type that became much more predominant in the *tup1(S649F)* mutant (Supplementary Figure S3A). These genomic results demonstrate that decreased Tup1 protein stability did not cause a simple loss of occupancy uniformly across the genome, but paradoxically resulted in many

regions of increased association. Thus, the *tup1(S649F)* mutant is clearly distinct from a *tup1* null.

The majority of Tup1 peaks in both wild type and mutant were located within intergenic regions, as expected (770/1266, 60%; [Supplementary Figure S3B](#)). Approximately 24% of peaks were located predominantly over UTRs and/or ORFs. Another 16% overlapped tRNA and other Pol III genes (*RPR1*, *SCR1*) and snRNAs. Peaks in intergenic regions displayed a range of \log_2 -fold changes in occupancy between *Tup1(S649F)* strains and wild-type *Tup1* strains, whereas most ORF and Pol III/snRNA locations showed decreased occupancy in the mutant relative to wild-type, even more so in α strains than in **a** strains ([Supplementary Figure S3C and D](#)). Occupancy over tRNA and snRNA genes was weak relative to the majority of *Tup1* peaks; therefore, it is uncertain what role *Tup1* plays at these loci ([Supplementary Figure S3C](#)). However, with over 50% of yeast tRNA genes showing occupancy of *Tup1* within our threshold parameters and a number of others with weaker but observable association in a genome browser, the occupancy of *Tup1* peaks at Pol III genes is unlikely to be coincidental.

Many genes with altered expression in the *tup1(S649F)* mutant are located downstream of a *Tup1* peak

Current models of *Tup1* function suggest it affects transcription by associating with target promoters and influencing their chromatin state and recruitment of factors. Thus, *Tup1* occupancy is expected within intergenic regions upstream of the genes that its complex directly regulates. To assess how many of the genes with altered expression in the *tup1(S649F)* mutant could be regulated by *Tup1* directly, we intersected the list of differentially expressed genes with those that had a *Tup1* peak located upstream of the ORF ([Table 2](#)). tRNA genes were excluded from this analysis due to their small size and inability to accurately map sequencing reads to specific loci. In both mating types, the majority of protein-coding genes that displayed increased expression in the mutant were located downstream of a *Tup1* peak (78% for **a**, 67% for α). Decreased expression changes appeared more likely to be indirect effects, at least in **a** strains, as the few genes with diminished expression in the mutant strains were not as likely to be associated with *Tup1* occupancy (29% in **a**, 56% in α). Overall, 75% of genes with altered expression in the *tup1(S649F)* mutant in **a** strains and 66% in α strains had an upstream *Tup1* peak, suggesting most transcriptional effects are a result of changes to the *Tup1* located within their promoters. A small number of genes with expression changes in both mating types had a *Tup1* peak located over the ORF; based on current models of *Tup1* function, it is not clear if or how *Tup1* could be regulating these genes directly.

Increased association of *Tup1(S649F)* correlates with increased expression of downstream genes

To examine patterns in occupancy changes between the strains, all of the *Tup1* peaks were merged into a single set and a mean enrichment score obtained for each strain, followed by k-means clustering of the data. This analysis identified groups of *Tup1* peak locations that displayed differences in occupancy between the wild-type and mutant strains. Four of the eight clusters in [Figure 7A](#) showed increased occupancy of *Tup1(S649F)* in both **a** and α strains (clusters 2, 4, 5, and 6), while two other clusters had diminished occupancy of the *Tup1(S649F)* relative to WT (clusters 3 and 8). The remaining two clusters appeared to have only minor or variable occupancy changes in *Tup1(S649F)* relative to wild

type (clusters 1 and 7). Intergenic peaks were disproportionately represented in the clusters in which occupancy appeared to increase in mutant relative to wild type (greater than 80% of the peaks; clusters 2,4,5, and 6; [Supplementary Table S6](#)). However, those clusters with diminished occupancy in mutant relative to wild type had many fewer intergenic peaks (23% for cluster 3; 35% for cluster 8). Thus, locations that lost occupancy in the mutant tended to be those with occupancy in nonintergenic locations, whereas those that gained occupancy in the mutant tended to be within intergenic positions from which they could influence the expression of downstream target genes.

We next investigated the relationship between changes in *Tup1* association and gene expression changes in *tup1(S649F)* vs wild type. For this analysis, we considered only genes that are located downstream of *Tup1* peaks and used the ChIP k-means clusters as a method to divide the large number of gene points into smaller groups for easier interpretation, while also highlighting the differences among clusters. \log_2 fold change in RNA expression was plotted vs \log_2 fold change in *Tup1* occupancy for individual gene/peak combinations ([Supplementary Figures S4 and S5](#)). Each gene was then categorized as “Up” or “Down” for both ChIP occupancy and RNA expression if the absolute change was greater than 1.5-fold change, otherwise as “NC” (No Change). The simplified heat maps in [Figure 7B](#) allow visualization of which occupancy and expression combinations were most prevalent in each cluster, when comparing mutant and wild-type strains with an α mating type. Each of the nine squares represents a unique combination of “Up,” “NC,” or “Down,” in *Tup1* occupancy and in gene expression. Notably, none of the clusters had significant numbers of genes in the upper right square, which would indicate increased *Tup1* occupancy and decreased expression, an expectation for a strict corepressor. Instead, increases in occupancy often occurred concomitantly with increased expression. In clusters 2, 4, 5, and 6, the upper left square had a substantial number of genes (genomic snapshot examples of clusters 4 and 6 peaks are in [Figure 7C](#)). Clusters 1 and 8, as expected, showed the largest proportion of genes in the central square, representing no significant changes either in occupancy or expression levels (example of cluster 8 peak in [Figure 7C](#)). Finally, cluster 3, which exhibited mostly decreases in *Tup1* occupancy, had very few changes in gene expression. Again, this does not agree with the prediction for a corepressor, in which diminished association with the promoter would be expected to increase expression of target genes. Similar results were obtained for **a** strains ([Supplementary Figure S6](#)).

Overall, those clusters which exhibited increased occupancy of *Tup1* (2, 4, 5, 6) had the largest proportion of downstream genes with significantly altered expression levels, approximately 50–60% ([Figure 7D](#)), with the vast majority of those changes representing increased expression ([Supplementary Figures S4 and S5 and Table S7](#)). Considering that our analysis was performed in rich media conditions in logarithmically growing cells representing all stages of the cell cycle, this level of positive correlation between *Tup1* occupancy and gene expression is likely significant. The actual number of genes displaying changes in occupancy and expression may be higher than the numbers reported here; viewing the genes as individual points revealed that genes within the “No Change” category often displayed minor alterations in occupancy and expression ([Supplementary Figures S4 and S5](#)). These results suggest that while the *Tup1(S649F)* protein is less abundant and less stable than wild type, it associates strongly with many genic loci with increased expression. Thus, many of the RNA expression changes observed at locations downstream

of Tup1 peaks may be a direct result of Tup1(S649F) mutant properties.

The *tup1(S649F)* α strain fails to downregulate critical **a**-specific genes

The mating irregularities and shmoo phenotype of the *tup1(S649F)* α strain suggest misregulation of the genes normally expressed in only one of the two haploid mating types. The three *S. cerevisiae* cell types, haploid **a** cells, haploid α cells, and **a**/ α diploid cells, each have distinct patterns of mating-type-specific transcription (Haber 2012). Genes specific to the **a** mating type are activated in **a** cells by Mcm1 (Elble and Tye 1991). In α cells and **a**/ α diploids, Mcm1 heterodimerizes with $\alpha 2$ to form a repressor that turns off the expression of these **a**-specific genes (Johnson and Herskowitz 1985; Keleher et al. 1988). Haploid-specific genes, such as *HO*, are repressed in diploids by a heterodimeric **a**1/ $\alpha 2$ repressor (Goutte and Johnson 1988; Keleher et al. 1988). Repression by both Mcm1/ $\alpha 2$ and **a**1/ $\alpha 2$ is dependent on Tup1 (Keleher et al. 1992). An altered function of Tup1 in haploid cells could therefore lead to aberrant expression of **a**-specific genes in the α cells.

To investigate this prediction, we first used the RNA-Seq analysis to identify genes that were differentially expressed between **a** and α haploid cells. Only 13 genes showed an expression change greater than twofold between the mating types in wild type. These genes are listed in Supplementary Table S9 and include those encoding the **a** and α mating pheromones [MFA1, MFA2, MF(ALPHA)1, MF(ALPHA)2], the receptors for **a**- and α -factor (STE3, STE2), and other genes encoding proteins involved in the pheromone response. The volcano plots in Figure 8A, which display significance vs fold change, highlight the changes in these 13 genes between the two mating types (noted with gene common names). Genes noted on the left side of the graph are **a**-specific genes that were downregulated in α cells (MFA1, MFA2, BAR1, STE2, STE6, and AGA2), and genes noted on the right side of the graph are α -specific genes that were expressed only in α cells [MF(ALPHA)1, MF(ALPHA)2, STE3, AFB1, SAG1, PRM7, and BSC1]. These results are consistent with prior studies that have examined differential expression between **a** and α cells, with the addition of BSC1 and PRM7 that have smaller transcriptional effects (but still above the twofold threshold; Galgoczy et al. 2004). BSC1 and PRM7 should be considered as a single gene for our analyses, as the two comprise a continuous ORF, IMI1, in W303 strains (but they are separate genes in the S288C reference strain and are listed separately in Supplementary Tables S3, S4, and S7).

The plot for *tup1(S649F)* α vs **a** strains is strikingly different and illustrates that many more genes showed differential expression between the mating types in the mutant relative to wild type (Figure 8A, Right). A large number of genes appeared on the right side of the graph, indicating increased expression in α cells relative to **a** cells. A smaller number of genes appeared on the left side of the graph; these genes that showed diminished expression in α cells did not have changes that were as dramatic as those that increased on the right side. The 13 genes with differential expression in wild type **a** and α cells are also indicated with their common names on the *tup1(S649F)* plot. Consistent with the expectation that Tup1 represses expression of **a**-specific genes, the six **a**-specific genes that are normally substantially downregulated in α cells were either less downregulated (STE2, STE6, and MFA2) or were now upregulated (BAR1, MFA1, and AGA2) in *tup1(S649F)* α cells (bold purple-boxed genes in Figure 8A; fold change α vs **a** for wild type and mutant listed in Supplementary Table S9). Only 20% of the genes, we found to be aberrantly

differentially expressed in *tup1(S649F)* α also displayed changes in gene expression in a *tup1* null α strain (Chen et al. 2013).

GO analysis of genes with altered expression in *tup1(S649F)* α vs *tup1(S649F)* **a** identified most of the same categories that were previously found in the comparison of *tup1(S649F)* α to wild-type α that were unique to α strains (Supplementary Table S5). The percentage of genes involved in aspects of mating, including conjugation with cellular fusion and response to pheromone, increased in the *tup1(S649F)* α vs *tup1(S649F)* **a** pool relative to the comparison to wild-type α and therefore had much more significant *P*-values; this was not true of the other α -specific gene sets. Manual examination and curation of the genes that became differentially regulated between α and **a** strains in the *tup1(S649F)* mutant identified a few additional genes involved in various aspects of mating, for 18 total genes (in addition to the 13 that change in WT **a** vs α cells, total = 31; Supplementary Table S9). Thus, the pool of genes regulated by Tup1 that are involved in mating appears to extend beyond the set of traditionally defined **a**-specific genes. The promoters of these additional genes appear to be distinct from the **a**-specific genes because they are not bound by $\alpha 2$ (Galgoczy et al. 2004), at least not at the level of the **a**-specific promoters or within the defined threshold parameters. All but two of them did not have Tup1 occupancy above our threshold of detection in wild-type **a** or α strains. However, five more had detectable Tup1(S649F) occupancy in the α strain. While expression changes for these few genes could be directly due to Tup1(S649F) occupancy within their promoters, the majority of changes appear to be indirect effects. Nevertheless, aberrant expression of these additional genes may contribute to the α -specific mating irregularities and growth defect observed in the *tup1(S649F)* mutant.

Wild-type Tup1 binds upstream of some expressed mating-type-specific genes

We expected the wild-type Tup1 ChIP-Seq to show occupancy of Tup1 upstream of **a**-specific genes in the α strain, as Tup1 is required for repression of these genes via Mcm1/ $\alpha 2$ (Keleher et al. 1992). However, only two promoters, those of STE6 and BAR1, behaved as predicted, with stronger Tup1 occupancy in the α strain than in the **a** strain (Figure 8B, Supplementary Figure S7). MFA2 and STE2 displayed the opposite pattern and had a larger amount of upstream Tup1 in the **a** strain in which the gene is expressed rather than repressed. The final two genes, AGA2 and MFA1, had similar occupancy in **a** and α strains (MFA1 is not shown in Figure 8B because it fell below the threshold detection of our peak calling program, but very weak occupancy could be seen visually in a genome browser; Supplementary Figure S7). Tup1 occupancy within the promoters of the **a**-specific genes was generally weak, with the exception of occupancy upstream of MFA2 in the **a** cell, and failed to correlate with the dramatic difference in RNA expression observed for these genes between the **a** and α strains (Figure 8B, Supplementary Figure S7 and Table S9). Thus, Tup1 did not show the differential association at **a**-specific promoters between mating types predicted by the long-standing model that Tup1-Cyc8 is recruited to these promoters in α cells for repression via $\alpha 2$.

The α -specific genes were not necessarily expected to display upstream Tup1 occupancy, since their differential expression between **a** and α strains is driven by the presence of the $\alpha 1$ activator specifically in α cells rather than by repression in **a** cells (Strathern et al. 1981). However, MF(ALPHA)1, MF(ALPHA)2, SAG1, and BSC1/PRM7 all showed upstream Tup1 occupancy in at least one strain (Figure 8B, Supplementary Figure S7). The Tup1 signal

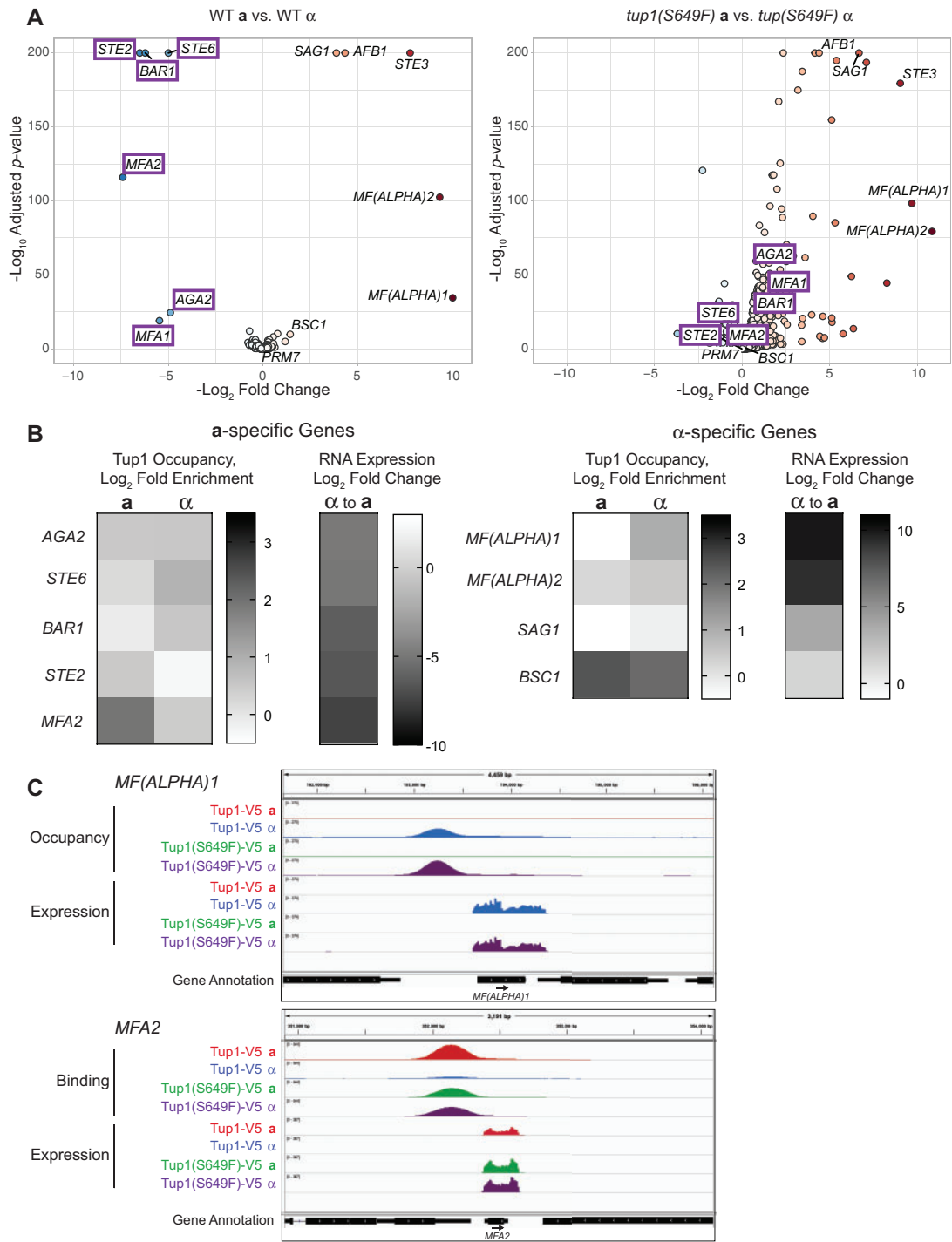


Figure 8 Regulation of mating-type genes is altered in the *tup1(S649F)* mutant. (A) Many more genes show differential regulation between *a* and α mating types in the *tup1(S649F)* mutant than in wild type. Volcano plots of RNA-Seq data show expression differences between *a* and α strains for wild type (Left) and the *tup1(S649F)* mutant (Right). The $-\log_{10}$ adjusted P-values were plotted relative to the \log_2 fold change for all genes ($n = 5730$). Each dot represents a single gene; those with increased or decreased expression are shown as deepening shades of red or blue, respectively. The 13 genes identified with their common name are differentially regulated greater than twofold between the wild-type *a* and α strains. The six *a*-specific genes that lose their differential expression between mating types in the *tup1(S649F)* mutant are boxed in purple. (B) Tup1 occupancy at mating-type-specific genes does not predict RNA expression changes. Shown are heat maps indicating \log_2 -fold enrichment of Tup1 occupancy and \log_2 -fold change in RNA expression at *a*- (Left) and α -specific genes (Right). Color scales are shown to the right of each heat map. Only genes with detectable ChIP-Seq peaks in wild-type *a* and/or α strains are shown. Genome browser snapshots for all genes are shown in [Supplementary Figure S7](#), and numerical values are listed in [Supplementary Table S9](#). (C) *MF(ALPHA)1* and *MFA2* unexpectedly display upstream Tup1 occupancy in the mating-type strain in which the gene is expressed rather than repressed. Snapshots of ChIP-Seq (Occupancy) and RNA-Seq (Expression) results from the IGV genome browser (Broad Institute) show the sequenced fragment pileups for Tup1 peaks in the intergenic regions upstream of *MF(ALPHA)1* and *MFA2*. Tracks represent an average of three biological samples for each strain. The four strains for each experiment were autoscaled as a group for occupancy and expression separately to account for differences in fragment depth between locations. Colors for both ChIP-Seq and RNA-Seq are as follows: Tup1-V5 WT *a* (red), Tup1-V5 WT α (blue), Tup1(S649F)-V5 *a* (green) and Tup1(S649F)-V5 α (purple). The bottom track displays gene annotations.

upstream of *BSC1/PRM7* appears as 2–3 peaks and is the strongest of all **a**- and α -specific genes. The entire group of mating-type-specific genes, both **a**- and α -specific, therefore, shows a range of Tup1 occupancy within their promoters, rather than the expected Tup1 association upstream of only the **a**-specific genes in α cells.

Most intriguing among the mating-type-specific genes were the **a**-specific gene *MFA2* and the α -specific gene *MF(ALPHA)1*. Both of these promoters exhibited strong Tup1 occupancy in the mating type in which the gene is strongly expressed [**a** for *MFA2* and α for *MF(ALPHA)1*; Figure 8C]. *MFA2* also displayed Tup1 occupancy in the α cell, as expected, but the association was weaker than in the **a** cell. In the *tup1(S649F)* mutant, the *MFA2* promoter showed strong occupancy of Tup1 in both **a** and α cells and a loss of differential RNA expression between the two mating types. Tup1 occupancy and RNA expression of α -specific genes *BSC1/PRM7*, *SAG1*, and *MF(ALPHA)2* all increased in the α strain in the *tup1(S649F)* mutant (Supplementary Figure S7 and Table S9). Collectively, these results suggest Tup1 and Tup1(S649F) could act as a coactivator at some of the mating-type genes. The critical distinction is that for *MFA2* and *MF(ALPHA)1*, we observed this coactivator function as a feature of wild-type differential expression between mating types, suggesting that even in a wild-type cell, Tup1 shows properties consistent with coactivator function. These results are difficult to reconcile with current models of Tup1 repression of **a**/ α regulation and suggest the role of Tup1 at these genes may be different than previously hypothesized.

Discussion

The Tup1-Cyc8 complex was originally defined as a corepressor due to its ability to decrease transcription when tethered upstream of reporter genes. However, increasing evidence shows that Tup1 and Cyc8 display properties of coactivators in certain contexts, suggesting the complex would be more aptly termed a coregulator. We present here two additional observations that contribute to the body of evidence suggesting coactivator function of Tup1-Cyc8. First, increased occupancy of the Tup1(S649F) mutant protein is correlated with upregulation of downstream target genes. Second, occupancy of wild-type Tup1 upstream of two mating-type-specific genes, *MFA2* and *MF(ALPHA)1*, occurs within the strain in which the gene is expressed rather than in the strain in which the gene is repressed. These points necessitate re-evaluation of models of how Tup1 functions and the mechanisms responsible for mating-type-specific gene expression.

The *tup1(S649F)* mutant appears to favor the coactivator state

Based on the reduction in protein level in the *tup1(S649F)* strain and phenotypes that are similar to, but not as severe as, a *tup1* null, we believe *tup1(S649F)* is a hypomorphic allele. This mutation is fully recessive and thus unlikely to be a neomorph, which is usually dominant. When considering the RNA-Seq results, *tup1(S649F)* behaves as expected for a simple corepressor mutation, as most genes show increased expression relative to wild type (Figure 5). However, the addition of Tup1 occupancy data from ChIP-Seq presents a more complex picture, in which increased gene expression is observed even at locations in which the mutant protein is more abundant than the wild-type protein (Figure 7). We suggest that at some promoters, the *tup1(S649F)* mutant not only has reduced ability to perform its corepressor function but has shifted toward its coactivator state. When compared to wild type, many fewer genes exhibit decreased

expression in a *tup1(S649F)* mutant than in a *tup1* null, a distinction that is consistent with retention of a coactivator function by *tup1(S649F)* (Chen et al. 2013).

The preference of Tup1(S649F) for the coactivator state could be explained by reduction or loss of its association with DNA-binding recruiter proteins at many target promoters. Several studies point to disruption of this interaction between Tup1-Cyc8 and its DNA-binding partner as a mechanism by which the complex is converted from a corepressor to a coactivator, often via phosphorylation of the DNA-binding protein (Papamichos-Chronakis et al. 2002; Proft and Struhl 2002; Papamichos-Chronakis et al. 2004; Roy et al. 2014). Tup1-Cyc8 remains at these promoters and aids in the recruitment of complexes such as SAGA and SWI/SNF that promote gene activation. Different sets of genes are controlled by distinct DNA-binding factors and are responsive to different kinases, illustrating that each pathway has developed its unique method of alternating between repressive and activating states.

A similar mechanism for corepressor to coactivator conversion may occur at genes regulated by $\alpha 2$ -Tup1. At the *STE2* and *STE6* **a**-specific promoters, Tup1-Cyc8 remains bound upon removal of $\alpha 2$ and is important for Gcn5-dependent acetylation and rapid de-repression (Desimone and Laney 2010), suggesting Tup1 can act as a coactivator in the absence of $\alpha 2$. Our observation of Tup1 occupancy at the *MFA2* promoter in both **a** and α cells is consistent with this hypothesis. In the α cell, $\alpha 2$ -Tup1 interaction would repress expression of *MFA2*, but in the **a** cell, the absence of $\alpha 2$ would allow Tup1 to exist in its coactivator form, promoting expression of *MFA2*. Based upon previous studies, the position of the *tup1(S649F)* mutation could be expected to decrease or eliminate interaction with the $\alpha 2$ repressor protein (Komachi and Johnson 1997). The simultaneous increase in both *MFA2* expression and Tup1(S649F) occupancy upstream of *MFA2* in both **a** and α *tup1(S649F)* cells is therefore also consistent with this model (Supplementary Figure S7). Likewise, the previous observation that a WD domain deletion mutant of Tup1 had a stronger de-repressive effect on *MFA2* than a *tup1* null (Komachi and Johnson 1997; Zhang et al. 2002) can be explained by a dual corepressor/coactivator function at *MFA2*. A *tup1* null constitutes a loss of both functions, whereas the disrupted $\alpha 2$ interaction caused by WD deletion or S649F mutation might affect only corepressor function. Since these mutants appear to retain coactivator capacity, they would lead to higher expression of target genes than a *tup1* null.

Genomic redistribution of Tup1 occupancy in the *tup1(S649F)* mutant supports a change in the protein(s) that retain Tup1 at promoters

The types of genome-wide changes in Tup1 occupancy observed in the *tup1(S649F)* mutant relative to wild type and the wide variety of genes with altered expression suggest that this mutation affects the association of Tup1 not only with $\alpha 2$ but with additional DNA-binding proteins (Supplementary Tables S4 and S5). Our ChIP-Seq data demonstrated the reduction in Tup1 occupancy at some locations in the *tup1(S649F)* mutant, and a gain at even more locations (Figure 6, B and C). At a number of sites, Tup1 had barely detectable association in wild type but substantial occupancy in the mutant, and some peaks shifted relative to their original location (Supplementary Figure S3A). Since Tup1 does not associate directly with DNA, these alterations imply a change in affinity of Tup1(S649F) for the proteins that tether it to DNA. The *tup1(S649F)* mutation could specifically affect the relevant WD domain-binding interface necessary for these

interactions or could affect the association of more N-terminal repression domains with DNA-binding proteins due to a general loss of protein stability. The *tup1(S649F)* mutant could therefore represent on a genome-wide scale what has been observed previously at individual genes that reduction or loss of interaction with the DNA-binding recruiter shifts Tup1 to a coactivator form but does not eliminate its association with chromatin. Our observation of substantially less Tup1 occupancy upstream of *MFA2* at the repressed gene (α cell) than at the active gene (**a** cell) also raises the possibility that interaction with DNA-binding proteins such as $\alpha 2$ could dampen the amount of Tup1 at the promoter. If so, this may be another factor contributing to locations of increased occupancy of Tup1(S649F) across the genome.

The most perplexing aspect of this model is the mechanism by which Tup1 is retained at promoters to facilitate gene activation in the absence of the interaction with the original DNA-binding recruiter protein. The answer may lie in the observation that Tup1 localizes within wide nucleosome depleted regions that have binding sites for many factors (Rizzo et al. 2011; Parnell et al. 2020), and promoters often show redundancy of recruitment of Tup1 by multiple DNA-binding proteins (Hanlon et al. 2011). In this way, Tup1-regulated gene promoters behave more like higher eukaryotic enhancers than most yeast promoters and are capable of responding to input from multiple cellular conditions simultaneously (Hanlon et al. 2011; Rizzo et al. 2011). Loss of interaction with one DNA-binding protein may be critical for the switch to a coactivator state, but another could ensure retention of Tup1-Cyc8 at the promoter. Alternatively, once recruited to a promoter, Tup1 could remain associated by virtue of interaction with a more general protein, such as histones or the HMG-containing protein Nhp6, both shown to bind to Tup1 and/or Cyc8 under certain conditions (Laser et al. 2000; Fragiadakis et al. 2004). Given the large number of proteins with which Tup1 and Cyc8 are capable of forming interactions, including histone deacetylases and components of the Mediator complex (Kuchin and Carlson 1998; Gromoller and Lehming 2000; Papamichos-Chronakis et al. 2000; Watson et al. 2000; Han et al. 2001; Davie et al. 2003), many other scenarios are possible. This complexity highlights the importance of studying genes in their natural context and the limitations of reporter-based experiments in which transcription factor binding sites are isolated from other factors that normally influence their interaction with complexes such as Tup1-Cyc8.

The role of Tup1 in the regulation of mating-type-specific RNA expression extends beyond repression of **a**-specific genes.

Our results question the simplicity of the long-standing model that Tup1-Cyc8 association with $\alpha 2$ /Mcm1 at **a**-specific promoters causes their repression in α cells. Despite the dramatic differences in **a**-specific gene expression between **a** and α cells and between wild type and *tup1(S649F)* mutant α cells, most promoters for these genes lacked substantial Tup1 occupancy or did not display the expected differential in Tup1 occupancy between **a** and α cells (Figure 8, Supplementary Figure S7). Most surprisingly, we observed strong association of Tup1 with the *MFA2* promoter within the **a** cell in which the gene is expressed, suggesting Tup1 could participate in activation as well as repression of *MFA2* within different cellular contexts. Another **a**-specific gene, *STE6*, requires Tup1 for full expression (Desimone and Laney 2010), raising the possibility that a coactivator function of Tup1 is required for activation of some of the **a**-specific genes.

While Tup1 has not previously been suggested to regulate α -specific genes, we observed Tup1 occupancy within the promoters of these genes at levels similar to or higher than those at

the **a**-specific genes (Figure 8, Supplementary Figure S7). Similar to *MFA2*, strong Tup1 association was observed upstream of the α -specific gene *MF(ALPHA)1* within the α cell in which the gene is expressed, suggesting a role for Tup1 in gene activation. The promoters of *MF(ALPHA)2*, *SAG1*, and *BSC1/PRM7* exhibit increased occupancy of Tup1(S649F) as well as increased expression in the α strain or in both mating types, further supporting a positive correlation between Tup1 occupancy and expression of the α -specific genes. Consistent with this idea, the group of α -specific genes, including *MF(ALPHA)1*, collectively display diminished expression in a *tup1* null (Chen et al. 2013; Supplementary Table S9).

Additional evidence for a coactivator role for Tup1 at these genes can be found in a former study of gene expression in a *tup1* null strain (Chen et al. 2013). Comparison of gene expression in *tup1* null and wild-type *MAT α* strains in the S288c background revealed a decrease in expression of α -specific genes in the *tup1* null (Supplementary Table S10), a result that is fully consistent with the concept that Tup1 can act as a coactivator at some genes. We did not use a *tup1* null in our studies because in our W303 background the null is extremely sick and develops suppressors, leading to inconsistencies in gene expression results (Figure 2B). However, comparison of our *tup1(S649F)* data with the *tup1* null data of Chen et al. (2013) revealed different effects of these alleles on both α -specific genes and the new class of mating-related genes affected by *tup1(S649F)* (Supplementary Tables S8 and S9). Even though there are significant differences in strain background and methodologies (RNA-Seq vs microarray), it is clear that the *tup1(S649F)* and *tup1* null alleles have markedly different effects on the expression on these classes of genes in *MAT α* cells.

Our results therefore present a perplexing conundrum regarding the nature of Tup1 regulation of the mating-type-specific genes, as upstream Tup1 occupancy did not necessarily predict its effects on transcription. In some cases, the association of Tup1 appears to argue for an activator role of Tup1, but at other genes, occupancy does not necessarily correlate with expression levels, particularly when considering repression of the **a**-specific genes. The strongest transcriptional effects of the *tup1(S649F)* mutant were observed at these **a**-specific genes, yet occupancy of Tup1 was not substantially altered. Perhaps some of the effects of Tup1 on expression could occur indirectly via its regulation of other transcription factors, a number of which display Tup1 occupancy within their upstream regions. Given the complex nature of promoters regulated by Tup1, additional as yet uncharacterized factors at these locations likely act in conjunction with or in opposition to Tup1, making it difficult to discern the direct relationship between Tup1 occupancy and expression levels. Nevertheless, the results presented here highlight that Tup1 likely plays a dual role in the regulation of mating type in yeast, having the capacity to function as either a coactivator or a corepressor at different genes or in different mating types. The role of Tup1 in the regulation of mating-type-specific genes is, therefore, both more complex and more comprehensive than previously appreciated, and much remains to be learned about the nature of how Tup1-Cyc8 affects transcriptional processes.

Acknowledgments

The authors thank Tim Formosa and members of the Stillman lab for advice throughout the course of these experiments and Tim Formosa for comments on the manuscript. They thank high school summer students Micah Spjute and Ellie Siddoway for

help with genetic screens for *tup1* mutants. Plasmid pFW45 containing the *TUP1* gene was provided by Robert Trumbly, and plasmid pZC03 (pFA6a-TEV-6xGly-V5-HIS3MX) was provided by Zaily Connell and Tim Formosa.

Funding

This work was supported by National Institutes of Health grant GM-121079 awarded to D.J.S.

Data availability

Strains and plasmids are available upon request. [Supplementary Table S1](#) lists the strains used in this study. Primers used for RT-qPCR and ChIP qPCR analysis are listed in [Supplementary Table S2](#). RNA-Seq differential expression data are shown in [Supplementary Table S3](#); genes with greater than twofold change are listed in [Supplementary Table S4](#), along with the cluster in which they were placed ([Figure 5B](#)). All ChIP-Seq peaks with location and cluster information ([Figure 7A](#)) are listed in [Supplementary Table S8](#); flanking genes associated with each are also indicated. RNA-Seq and ChIP-Seq data have been deposited in NCBI's Gene Expression Omnibus with the accession number GSE173722. [Supplementary material](#) is available at figshare: <https://doi.org/10.25386/genetics.14829171>.

Conflicts of interest

The authors declare that there is no conflict of interest.

Literature cited

- Adams GE, Chandru A, Cowley SM. 2018. Co-repressor, co-activator and general transcription factor: the many faces of the Sin3 histone deacetylase (HDAC) complex. *Biochem J.* 475:3921–3932.
- Ausubel FM, Brent R, Kingston RE, Moore DE, Seidman JG, et al. 1987. *Current Protocols in Molecular Biology*. New York: Wiley and Sons.
- Bhoite LT, Yu Y, Stillman DJ. 2001. The Swi5 activator recruits the Mediator complex to the *HO* promoter without RNA polymerase II. *Genes Dev.* 15:2457–2469.
- Bobola N, Jansen RP, Shin TH, Nasmyth K. 1996. Asymmetric accumulation of Ash1p in postanaphase nuclei depends on a myosin and restricts yeast mating-type switching to mother cells. *Cell.* 84:699–709.
- Carrico PM, Zitomer RS. 1998. Mutational analysis of the Tup1 general repressor of yeast. *Genetics.* 148:637–644.
- Chen G, Courey AJ. 2000. Groucho/TLE family proteins and transcriptional repression. *Gene.* 249:1–16.
- Chen K, Wilson MA, Hirsch C, Watson A, Liang S, et al. 2013. Stabilization of the promoter nucleosomes in nucleosome-free regions by the yeast Cyc8-Tup1 corepressor. *Genome Res.* 23:312–322.
- Conlan RS, Gounalaki N, Hatzis P, Tzamarias D. 1999. The Tup1-Cyc8 protein complex can shift from a transcriptional co-repressor to a transcriptional co-activator. *J Biol Chem.* 274:205–210.
- Cosma MP, Tanaka T, Nasmyth K. 1999. Ordered recruitment of transcription and chromatin remodeling factors to a cell cycle- and developmentally regulated promoter. *Cell.* 97:299–311.
- Davie JK, Edmondson DG, Coco CB, Dent SY. 2003. Tup1-Ssn6 interacts with multiple class I histone deacetylases in vivo. *J Biol Chem.* 278:50158–50162.
- DeRisi JL, Iyer VR, Brown PO. 1997. Exploring the metabolic and genetic control of gene expression on a genomic scale. *Science.* 278:680–686.
- Desimone AM, Laney JD. 2010. Corepressor-directed preacetylation of histone H3 in promoter chromatin primes rapid transcriptional switching of cell-type-specific genes in yeast. *Mol Cell Biol.* 30:3342–3356.
- Dranginis AM. 1990. Binding of yeast $\alpha 1$ and $\alpha 2$ as a heterodimer to the operator DNA of a haploid-specific gene. *Nature.* 347:682–685.
- Elble R, Tye BK. 1991. Both activation and repression of a-mating-type-specific genes in yeast require transcription factor Mcm1. *Proc Natl Acad Sci U S A.* 88:10966–10970.
- Fisher AL, Caudy M. 1998. Groucho proteins: transcriptional corepressors for specific subsets of DNA-binding transcription factors in vertebrates and invertebrates. *Genes Dev.* 12:1931–1940.
- Fragiadakis GS, Tzamarias D, Alexandraki D. 2004. Nhp6 facilitates Aft1 binding and Ssn6 recruitment, both essential for *FRE2* transcriptional activation. *EMBO J.* 23:333–342.
- Galgoczy DJ, Cassidy-Stone A, Llinas M, O'Rourke SM, Herskowitz I, et al. 2004. Genomic dissection of the cell-type-specification circuit in *Saccharomyces cerevisiae*. *Proc Natl Acad Sci U S A.* 101:18069–18074.
- Gietz RD, Sugino A. 1988. New yeast-*Escherichia coli* shuttle vectors constructed with in vitro mutagenized yeast genes lacking six-base pair restriction sites. *Gene.* 74:527–534.
- Gligoris T, Thireos G, Tzamarias D. 2007. The Tup1 corepressor directs Htz1 deposition at a specific promoter nucleosome marking the *GAL1* gene for rapid activation. *Mol Cell Biol.* 27:4198–4205.
- Gounalaki N, Tzamarias D, Vlasi M. 2000. Identification of residues in the TPR domain of Ssn6 responsible for interaction with the Tup1 protein. *FEBS Lett.* 473:37–41.
- Goutte C, Johnson AD. 1988. A1 protein alters the DNA-binding specificity of $\alpha 2$ repressor. *Cell.* 52:875–882.
- Grbavec D, Lo R, Liu Y, Greenfield A, Stifani S. 1999. Groucho/transducin-like enhancer of split (TLE) family members interact with the yeast transcriptional co-repressor Ssn6 and mammalian Ssn6-related proteins: implications for evolutionary conservation of transcription repression mechanisms. *Biochem J.* 337:13–17.
- Grbavec D, Lo R, Liu Y, Stifani S. 1998. Transducin-like Enhancer of split 2, a mammalian homologue of *Drosophila* Groucho, acts as a transcriptional repressor, interacts with Hairy/Enhancer of split proteins, and is expressed during neuronal development. *Eur J Biochem.* 258:339–349.
- Green SR, Johnson AD. 2004. Promoter-dependent roles for the Srb10 cyclin-dependent kinase and the Hda1 deacetylase in Tup1-mediated repression in *Saccharomyces cerevisiae*. *Mol Biol Cell.* 15:4191–4202.

- Gromoller A, Lehming N. 2000. Srb7p is a physical and physiological target of Tup1p. *EMBO J.* 19:6845–6852.
- Haber JE. 2012. Mating-type genes and MAT switching in *Saccharomyces cerevisiae*. *Genetics.* 191:33–64.
- Han SJ, Lee JS, Kang JS, Kim YJ. 2001. Med9/Cse2 and Gal11 modules are required for transcriptional repression of distinct group of genes. *J Biol Chem.* 276:37020–37026.
- Hanlon SE, Rizzo JM, Tatomer DC, Lieb JD, Buck MJ. 2011. The stress response factors Yap6, Cin5, Phd1, and Skn7 direct targeting of the conserved co-repressor Tup1-Ssn6 in *S. cerevisiae*. *PLoS One.* 6:e19060.
- Jabet C, Sprague ER, VanDemark AP, Wolberger C. 2000. Characterization of the N-terminal domain of the yeast transcriptional repressor Tup1. Proposal for an association model of the repressor complex Tup1 x Ssn6. *J Biol Chem.* 275:9011–9018.
- Jansen RP, Dowzer C, Michaelis C, Galova M, Nasmyth K. 1996. Mother cell-specific *HO* expression in budding yeast depends on the unconventional myosin Myo4p and other cytoplasmic proteins. *Cell.* 84:687–697.
- Johnson AD, Herskowitz I. 1985. A repressor (MAT alpha2 product) and its operator control expression of a set of cell type specific genes in yeast. *Cell.* 42:237–247.
- Keleher CA, Goutte C, Johnson AD. 1988. The yeast cell-type-specific repressor alpha 2 acts cooperatively with a non-cell-type-specific protein. *Cell.* 53:927–936.
- Keleher CA, Passmore S, Johnson AD. 1989. Yeast repressor a2 binds to its operator cooperatively with yeast protein Mcm1. *Mol Cell Biol.* 9:5228–5230.
- Keleher CA, Redd MJ, Schultz J, Carlson M, Johnson AD. 1992. Ssn6/Tup1 is a general repressor of transcription in yeast. *Cell.* 68:709–719.
- Kliewe F, Engelhardt M, Aref R, Schuller HJ. 2017. Promoter recruitment of corepressors Sin3 and Cyc8 by activator proteins of the yeast *Saccharomyces cerevisiae*. *Curr Genet.* 63:739–750.
- Knop M, Siegers K, Pereira G, Zachariae W, Winsor B, et al. 1999. Epitope tagging of yeast genes using a PCR-based strategy: more tags and improved practical routines. *Yeast.* 15:963–972.
- Kolde R. 2020. Implementation of heatmaps that offers more control over dimensions and appearance. <https://cran.r-project.org/package=pheatmap>.
- Komachi K, Johnson AD. 1997. Residues in the WD repeats of Tup1 required for interaction with alpha2. *Mol Cell Biol.* 17:6023–6028.
- Komachi K, Redd MJ, Johnson AD. 1994. The WD repeats of Tup1 interact with the homeo domain protein alpha 2. *Genes Dev.* 8:2857–2867.
- Kuchin S, Carlson M. 1998. Functional relationships of Srb10-Srb11 kinase, carboxy-terminal domain kinase CTDK-I, and transcriptional corepressor Ssn6-Tup1. *Mol Cell Biol.* 18:1163–1171.
- Laser H, Bongards C, Schuller J, Heck S, Johnsson N, et al. 2000. A new screen for protein interactions reveals that the *Saccharomyces cerevisiae* high mobility group proteins Nhp6A/B are involved in the regulation of the GAL1 promoter. *Proc Natl Acad Sci U S A.* 97:13732–13737.
- Lemontt JF, Fugit DR, Mackay VL. 1980. Pleiotropic mutations at the TUP1 locus that affect the expression of mating-type-dependent functions in *Saccharomyces cerevisiae*. *Genetics.* 94:899–920.
- Lin A, Du Y, Xiao W. 2020. Yeast chromatin remodeling complexes and their roles in transcription. *Curr Genet.* 66:657–670.
- Lipke PN, Hull-Pillsbury C. 1984. Flocculation of *Saccharomyces cerevisiae* tup1 mutants. *J Bacteriol.* 159:797–799.
- Longtine MS, McKenzie A, 3rd, Demarini DJ, Shah NG, Wach A, et al. 1998. Additional modules for versatile and economical PCR-based gene deletion and modification in *Saccharomyces cerevisiae*. *Yeast.* 14:953–961.
- Love MI, Huber W, Anders S. 2014. Moderated estimation of fold change and dispersion for RNA-seq data with DESeq2. *Genome Biol.* 15:550.
- Malave TM, Dent SY. 2006. Transcriptional repression by Tup1-Ssn6. *Biochem Cell Biol.* 84:437–443.
- Markert J, Luger K. 2021. Nucleosomes meet their remodeler match. *Trends Biochem Sci.* 46:41–50.
- Mennella TA, Klinkenberg LG, Zitomer RS. 2003. Recruitment of Tup1-Ssn6 by yeast hypoxic genes and chromatin-independent exclusion of TATA binding protein. *Eukaryot Cell.* 2:1288–1303.
- Muhlrad D, Hunter R, Parker R. 1992. A rapid method for localized mutagenesis of yeast genes. *Yeast.* 8:79–82.
- Mukai Y, Harashima S, Oshima Y. 1991. AAR1/TUP1 protein, with a structure similar to that of the beta subunit of G proteins, is required for a1-alpha 2 and alpha 2 repression in cell type control of *Saccharomyces cerevisiae*. *Mol Cell Biol.* 11:3773–3779.
- Narita T, Weinert BT, Choudhary C. 2019. Functions and mechanisms of non-histone protein acetylation. *Nat Rev Mol Cell Biol.* 20:156–174.
- Ng HH, Bird A. 2000. Histone deacetylases: silencers for hire. *Trends Biochem Sci.* 25:121–126.
- Nguyen PV, Hlavacek O, Marsikova J, Vachova L, Palkova Z. 2018. Cyc8p and Tup1p transcription regulators antagonistically regulate Flo11p expression and complexity of yeast colony biofilms. *PLoS Genet.* 14:e1007495.
- Nielsen PS, van den Hazel B, Didion T, de Boer M, Jorgensen M, et al. 2001. Transcriptional regulation of the *Saccharomyces cerevisiae* amino acid permease gene BAP2. *Mol Gen Genet.* 264:613–622.
- Papamichos-Chronakis M, Conlan RS, Gounalaki N, Copf T, Tzamarias D. 2000. Hrs1/Med3 is a Cyc8-Tup1 corepressor target in the RNA polymerase II holoenzyme. *J Biol Chem.* 275:8397–8403.
- Papamichos-Chronakis M, Gligoris T, Tzamarias D. 2004. The Snf1 kinase controls glucose repression in yeast by modulating interactions between the Mig1 repressor and the Cyc8-Tup1 co-repressor. *EMBO Rep.* 5:368–372.
- Papamichos-Chronakis M, Petrakis T, Ktistaki E, Topalidou I, Tzamarias D. 2002. Cti6, a PHD domain protein, bridges the Cyc8-Tup1 corepressor and the SAGA coactivator to overcome repression at GAL1. *Mol Cell.* 9:1297–1305.
- Parkhurst SM. 1998. Groucho: making its Marx as a transcriptional co-repressor. *Trends Genet.* 14:130–132.
- Parnell EJ, Parnell TJ, Yan C, Bai L, Stillman DJ. 2020. Ash1 and Tup1 dependent repression of the *Saccharomyces cerevisiae* HO promoter requires activator-dependent nucleosome eviction. *PLoS Genet.* 16:e1009133.
- Parnell EJ, Stillman DJ. 2019. Multiple negative regulators restrict recruitment of the SWI/SNF chromatin remodeler to the HO promoter in *Saccharomyces cerevisiae*. *Genetics.* 212:1181–1204.
- Parnell TJ. 2020. Multiple-replica multiple-condition Macs2 ChIPSeq wrapper. <https://github.com/HuntsmanCancerInstitute/MultiRepMacsChIPSeq>.
- Parnell TJ. 2021a. hciR package. <https://github.com/HuntsmanCancerInstitute/hciR>.
- Parnell TJ. 2021b. Yeast positioned nucleosomes. https://github.com/tjparnell/biotoolbox-nucleosome/blob/master/yeast_positioned_nucleosomes/SacCer3_R64_all_genes_NoDubious_UTR_chromo.gff3.gz.

- Proft M, Struhl K. 2002. Hog1 kinase converts the Sko1-Cyc8-Tup1 repressor complex into an activator that recruits SAGA and SWI/SNF in response to osmotic stress. *Mol Cell*. 9:1307–1317.
- Quinlan AR. 2020. bedtools: a powerful toolset for genome arithmetic. <https://bedtools.readthedocs.io/en/latest/>.
- Reyes AA, Marcum RD, He Y. 2021. Structure and function of ATP-dependent chromatin remodeling complexes. *J Mol Biol*. 433:166929.
- Rizzo JM, Mieczkowski PA, Buck MJ. 2011. Tup1 stabilizes promoter nucleosome positioning and occupancy at transcriptionally plastic genes. *Nucleic Acids Res*. 39:8803–8819.
- Rothstein R. 1991. Targeting, disruption, replacement, and allele rescue: integrative DNA transformation in yeast. *Meth Enzymol*. 194:281–302.
- Roy A, Jouandot D, 2nd, Cho KH, Kim JH. 2014. Understanding the mechanism of glucose-induced relief of Rgt1-mediated repression in yeast. *FEBS Open Bio*. 4:105–111.
- Shahbazian MD, Grunstein M. 2007. Functions of site-specific histone acetylation and deacetylation. *Annu Rev Biochem*. 76:75–100.
- Sherman F. 1991. Getting started with yeast. *Meth Enzymol*. 194:3–21.
- Sil A, Herskowitz I. 1996. Identification of asymmetrically localized determinant, Ash1p, required for lineage-specific transcription of the yeast HO gene. *Cell*. 84:711–722.
- Smith RL, Johnson AD. 2000. Turning genes off by Ssn6-Tup1: a conserved system of transcriptional repression in eukaryotes. *Trends Biochem Sci*. 25:325–330.
- Smith RL, Redd MJ, Johnson AD. 1995. The tetratricopeptide repeats of Ssn6 interact with the homeo domain of alpha 2. *Genes Dev*. 9:2903–2910.
- Soffers JHM, Workman JL. 2020. The SAGA chromatin-modifying complex: the sum of its parts is greater than the whole. *Genes Dev*. 34:1287–1303.
- Sprague ER, Redd MJ, Johnson AD, Wolberger C. 2000. Structure of the C-terminal domain of Tup1, a corepressor of transcription in yeast. *EMBO J*. 19:3016–3027.
- Stillman DJ. 2013. Dancing the cell cycle two-step: regulation of yeast G1-cell-cycle genes by chromatin structure. *Trends Biochem Sci*. 38:467–475.
- Storici F, Lewis LK, Resnick MA. 2001. In vivo site-directed mutagenesis using oligonucleotides. *Nat Biotechnol*. 19:773–776.
- Strathern J, Hicks J, Herskowitz I. 1981. Control of cell type in yeast by the mating type locus. The a1-a2 hypothesis. *J Mol Biol*. 147:357–372.
- Strathern JN, Klar AJ, Hicks JB, Abraham JA, Ivy JM, et al. 1982. Homothallic switching of yeast mating type cassettes is initiated by a double-stranded cut in the MAT locus. *Cell*. 31:183–192.
- Takahata S, Yu Y, Stillman DJ. 2009. FACT and Asf1 regulate nucleosome dynamics and coactivator binding at the HO promoter. *Mol Cell*. 34:405–415.
- Takahata S, Yu Y, Stillman DJ. 2011. Repressive chromatin affects factor binding at yeast HO (homothallic switching) promoter. *J Biol Chem*. 286:34809–34819.
- Tam J, van Werven FJ. 2020. Regulated repression governs the cell fate promoter controlling yeast meiosis. *Nat Commun*. 11:2271.
- Tanaka N, Mukai Y. 2015. Yeast Cyc8p and Tup1p proteins function as coactivators for transcription of Stp1/2p-dependent amino acid transporter genes. *Biochem Biophys Res Commun*. 468:32–38.
- Tellmann G. 2006. The E-Method: a highly accurate technique for gene-expression analysis. *Nat Methods*. 3:i-ii.
- Thomas BJ, Rothstein R. 1989. Elevated recombination rates in transcriptionally active DNA. *Cell*. 56:619–630.
- Tzamarias D, Struhl K. 1994. Functional dissection of the yeast Cyc8-Tup1 transcriptional co-repressor complex. *Nature*. 369:758–761.
- Tzamarias D, Struhl K. 1995. Distinct TPR motifs of Cyc8 are involved in recruiting the Cyc8-Tup1 corepressor complex to differentially regulated promoters. *Genes Dev*. 9:821–831.
- Varanasi US, Klis M, Mikesell PB, Trumbly RJ. 1996. The Cyc8 (Ssn6)-Tup1 corepressor complex is composed of one Cyc8 and four Tup1 subunits. *Mol Cell Biol*. 16:6707–6714.
- Verdone L, Caserta M, Mauro ED. 2005. Role of histone acetylation in the control of gene expression. *Biochem Cell Biol*. 83:344–353.
- Voth WP, Yu Y, Takahata S, Kretschmann KL, Lieb JD, et al. 2007. Forkhead proteins control the outcome of transcription factor binding by antiactivation. *EMBO J*. 26:4324–4334.
- Watson AD, Edmondson DG, Bone JR, Mukai Y, Yu Y, et al. 2000. Ssn6-Tup1 interacts with class I histone deacetylases required for repression. *Genes Dev*. 14:2737–2744.
- Wickner RB. 1974. Mutants of *Saccharomyces cerevisiae* that incorporate deoxythymidine-5'-monophosphate into deoxyribonucleic acid in vivo. *J Bacteriol*. 117:252–260.
- Williams FE, Trumbly RJ. 1990. Characterization of TUP1, a mediator of glucose repression in *Saccharomyces cerevisiae*. *Mol Cell Biol*. 10:6500–6511.
- Williams FE, Varanasi U, Trumbly RT. 1991. The CYC8 and TUP1 proteins involved in glucose repression in *Saccharomyces cerevisiae* are associated in a protein complex. *Mol Cell Biol*. 11:3307–3316.
- Wittwer CT, Reed GH, Gundry CN, Vandersteijn JG, Pryor RJ. 2003. High-resolution genotyping by amplicon melting analysis using LCGreen. *Clin Chem*. 49:853–860.
- Wolffe AP. 1996. Histone deacetylase: a regulator of transcription. *Science*. 272:371–372.
- Wong KH, Struhl K. 2011. The Cyc8-Tup1 complex inhibits transcription primarily by masking the activation domain of the recruiting protein. *Genes Dev*. 25:2525–2539.
- Zhang Z, Reese JC. 2004. Redundant mechanisms are used by Ssn6-Tup1 in repressing chromosomal gene transcription in *Saccharomyces cerevisiae*. *J Biol Chem*. 279:39240–39250.
- Zhang Z, Varanasi U, Trumbly RJ. 2002. Functional dissection of the global repressor Tup1 in yeast: dominant role of the C-terminal repression domain. *Genetics*. 161:957–969.

Communicating editor: C. Kaplan